João Miguel Rolo Silva

Licenciado em Ciências de Engenharia

de Micro e Nanotecnologias

Effect of eco-friendly solvents in solution-based AlO_x dielectrics at low temperature

Dissertação para obtenção do Grau de Mestre em
Engenharia de Micro e Nanotecnologias

Orientadora: Doutora Rita Maria Mourão Salazar Branquinho,

Prof. Auxiliar, FCT/UNL

Júri:

Presidente: Doutor Rodrigo Ferrão de Paiva Martins

Arguente: Doutora Ana Cláudia Madeira Botas Gomes Pimentel

Vogal: Doutora Rita Maria Mourão Salazar Branquinho

FACULDADE DE CIÊNCIAS E TECNOLOGIA
UNIVERSIDADE NOVA DE LISBOA

Dezembro, 2020

Effect of eco-friendly solvents in solution-based AlO_x dielectrics at low temperature

Faculdade de Ciências e Tecnologia

Universidade Nova de Lisboa

Acknowledgments

First of all, I would like to thank to the Faculty of Science and Technology from Universidade NOVA de Lisboa, for all the great experiences provided throughout my academic life.

I would like to acknowledge either to Professor Rodrigo Martins and Professor Elvira Fortunato for their hard work and commitment in the creation of the course of Micro and Nanotechnology and to gather great conditions to CENIMAT | I3N and CEMOP, which allow the realization of tests for my master thesis.

My most sincerely acknowledge goes to my thesis supervisor Professor Dr. Rita Branquinho, for all the guidance, hard work, remarkably advices and all the patience to deal with me. I would like to thank either to my monitor Emanuel Carlos, for teach me the lab techniques, how to improve my work easily and always for being a great human being.

I have to thank to all professors and colleagues that accompanied me during the academic life, for their expertise and share of knowledge, their funny moments and memories that I will take over life.

To my closest friends, I had to thank for pushing me and never letting me give up. They are one of my truth supports.

I want to thank my parents for always support my decisions and always giving me advices to have a successful life.

I would like to thank either to my both sisters for a home full of laughs and joy, which become all easier. I also want to thank to my closest family for being part of this step in my life and for all the supporting.

Abstract

Solution-based amorphous metal oxides have been lately used as one of the main options to develop transparent and flexible electronics with good performances at low cost. As time goes by, a necessity to preserve the environment emerged, so it is an urgent need to find eco-friendly materials. This work has the purpose of developing solution-based aluminium oxide (AlO_x) thin films using eco-friendly solvents and low temperature processes. Thin films structural and electrical properties were analysed and characterized systematically. Beyond, the application of these thin films as high-κ dielectrics in flexible substrates has been developed, once the low annealing temperatures become compactible with the flexible substrates. The electric properties of each thin film processed conditions were measured resorting to capacitors with a dimension of 0.2 mm^2. AlO_x capacitors with a 0.2 M concentration, 2-methoyethanol (2-ME) as solvent and an annealing temperature of 300 °C were developed. These devices showed a dielectric constant of 5.0 ± 0.2 and a leakage current of (1.8 ± 2.0) x 10^{-4} A/cm^2. Since, these standard capacitors use a health hazardous solvent, eco-friendly solvents such as 1-methoxy-2-propanol and ethanol were tested. They exhibited a dielectric constant of 7.9 ± 0.1 and 8.4 ± 0.1, respectively. However, the devices present a higher leakage current density compared to 2-ME capacitors. To apply them in flexible substrates a different method using a low thermal annealing at 150 °C assisted by DUV (deep-ultraviolet) irradiation for 60 minutes was performed. The resultant AlO_x devices presented a dielectric constant of 6.0 ± 0.3 at 1 kHz and a leakage current of (8.1 ± 9.9) x 10^{-4} A/cm^2 at 0.5 MV/cm. To finalize, as proof of concept, In_2O_3/AlO_x thin film transistors (TFTs) were successfully developed achieving better characteristics the devices annealed at 300 °C.

Keywords: Aluminum oxide, eco-friendly solvents, low temperature, high-κ dielectrics, flexible substrates, thin film transistors

Resumo

Os óxidos metálicos amorfos baseados em solução têm sido usados recentemente como uma das principais opções para desenvolver a eletrónica transparente e flexível com bom desempenho e baixo custo. Com o passar do tempo, surgiu a necessidade de preservar o meio ambiente, por isso é urgente encontrar materiais ecológicos. Este trabalho tem o objetivo de desenvolver filmes finos de óxido de alumínio (AlO_x) à base de solução utilizando solventes ecológicos e processos de baixa temperatura. As propriedades estruturais e elétricas dos filmes finos foram analisadas e caracterizadas sistematicamente. Além disso, a aplicação desses filmes finos como materiais de alta constante dielétrica (κ) em substratos flexíveis tem sido desenvolvida, uma vez que as baixas temperaturas de recozimento se tornam compatíveis com os substratos flexíveis. As propriedades elétricas de cada condição processada de filme fino foram medidas com recurso a condensadores com uma dimensão de 0.2 mm^2. Os condensadores de AlO_x com concentração de 0.2 M, 2-metoxietanol (2-ME) como solvente e temperatura de recozimento de 300 °C foram desenvolvidos. Esses dispositivos mostraram uma constante dielétrica de 5.0 ± 0.2 e uma corrente de fuga de (1.8 ± 2.0) ± 10^{-4} A/cm^2. Desde então, esses condensadores padrão usam um solvente perigoso para a saúde, solventes ecológicos, como 1-metoxi-2-propanol e etanol foram testados. Eles exibiram uma constante dielétrica de 7.9 ± 0.1 e 8.4 ± 0.1, respetivamente. No entanto, os dispositivos apresentam uma densidade de corrente de fuga maior em comparação com os condensadores com 2-ME. Para aplicá-los em substratos flexíveis, foi realizado um método diferente usando um recozimento térmico a baixa temperatura, 150 °C assistido por irradiação DUV (ultravioleta profundo) por 60 minutos. Os dispositivos de AlO_x resultantes apresentaram uma constante dielétrica de 6.0 ± 0.3 a 1 kHz e uma corrente de fuga de (8.1 ± 9.9) ± 10^{-4} A/cm^2 a 0.5 MV/cm. Para finalizar, como prova de conceito, os transístores de filme fino In_2O_3/AlO_x (TFTs) foram desenvolvidos com sucesso, alcançando melhores características que os dispositivos recozidos a 300 °C.

Palavras-chave: Óxido de alumínio, solventes ecológicos, baixas temperaturas, altas constantes dielétricas, substratos flexíveis, transístores de filme fino

List of Abbreviations

1-MP – 1-methoxy-2-propanol

2-ME – 2-methoxyethanol

AFM – Atomic Force Microscopy

ATR – Attenuated total reflectance

CEMOP – Centre of Excellence in Microelectronics and Optoelectronics Processes

CENIMAT – Centro de Investigação de Materiais

CCM – Conventional Combustion Method

Cf – Capacitance-frequency

CV – Capacitance-voltage

CVD – Chemical vapor deposition

DSC – Differential scanning calorimetry

DUV – Deep ultraviolet irradiation

FTIR – Fourier Transformed Infrared Spectroscopy

FUV – Far ultraviolet irradiation

GAXRD – Glancing angle X-ray diffraction

IPA – 2-isopropanol

IV – Current-voltage

JE – Current density-Breakdown electric field

LO – Longitudinal optical

MIM – Metal-Insulator-Metal

MIS – Metal-Insulator-Oxide

M-O – Metal Oxide

M-O-M – Metal Oxide Metal

NIR – Near-Infrared Spectroscopy

OV – Oxidizing reagent valency

PTFE - Polytetrafluoroethylene

PVD – Physical Vapor Deposition

R2R – Roll-to-roll

RC – Regenerated cellulose

rpm – Rotations per minute

RV – Reducing reagent valency

SCS – Solution Combustion Synthesis

SS – Subthreshold Swing

TFTs- Thin Film Transistors

TG – Thermogravimetry

TO – Transversal optical

UV – Ultraviolet

Vis – Visible

XRD – X-ray Diffraction

List of Symbols

A – area

c – concentration

C – capacitance

C_D – Depletion capacitance

C_{ox} – Oxide capacitance

C_t – Total capacitance

d – thickness

D – Drain

E – Breakdown electric field

eV – Electron volts

F – Farads

h – hour

I_{DS} – Current between drain and source

I_{OFF} – Drain current on the off status

I_{ON} – Drain current on the on status

J – Current density

k – Dielectric constant

L – Channel length

M - Molar

min – minute

q – charge

s - seconds

S – Source

V_{bias} – Bias voltage

V_{DS} – Voltage applied between drain and source

V_G – Voltage applied in the gate

V_{GS} – Voltage applied between gate and source

V_T – Threshold voltage

W – Channel width

°C – Celsius degrees

ΔE – Conduction band offset

ε_0 – Vacuum permittivity

μ_{sat} – Saturation mobility

α – Alpha

γ – Gamma

θ - Theta

φ – Redox stoichiometry

Ω - Ohm

Table of Contents

List of Figures

List of Tables

Motivation and Objectives

Research area of transparent electronics has gained lots of attention in the last decade. With the fast evolution of thin film transistors (TFTs), more demanding and new applications are emerging, such as flexible and wearable devices. Currently, the processes used to produce TFTs in large area have associated expensive methods and high cost.

Working on the development of solution-based AlO_x thin film dielectrics on TFTs using low cost processes and eco-friendly solvents are becoming competitive with the existing techniques. Alumina thin films has already performed great results by the research groups of CENIMAT and CEMOP, using 2-methoxyethanol (2-ME) as solvent. However, the challenge is on combining a greener solvent with low thermal annealing and achieve better results than obtained before.

So, the following tasks to reach the main objectives are:

- Production and characterization of solution-based AlO_x thin films gate dielectrics using 2-methoxyethanol (2-ME) and eco-friendly solvents;
- Optimization of solution-based AlO_x thin films gate dielectrics using eco-friendly solvents;
- Production and characterization of solution-based AlO_x thin films gate dielectrics on metal-insulator-metal (MIM) structures using flexible substrates;
- Application of optimized AlO_x gate dielectrics in solution-based TFTs.

1. Introduction

In the last decade, technology experienced a massive growing. Staring at this technological development, there has arisen a necessity for low-cost processes and eco-friendly materials that can contribute to a more sustainable world. Physical vapor deposition (PVD) and chemical vapor deposition (CVD) are the main techniques to produce thin films materials, however the requirements associated to high vacuums, temperatures and costs, [2] lead to the search for alternatives. Alternative materials to silicon started to be developed owing to the necessity for emerging applications in electronics like transparent flexible displays and large-area devices due to the lack of optical transparency and mechanical flexibility. As amorphous silicon presents performance limitations on these applications, new materials are required to the production of high-performance thin film transistors (TFT). Organic semiconductors, possess good transparency and flexibility, however they have some drawbacks like operational instability, low carrier mobility and environmental issues. [1], [3]–[5] Solution-processed amorphous metal oxides beyond solving these issues show a large area uniformity, a high dielectric constant and no need vacuum processes. Their solution processability have found new possibilities for low cost printable, as transparent devices in flexible substrates and roll to roll (R2R) processing techniques. Flexible, printable, disposable and transparent electronics have been deeply investigated as part of the solution. The main techniques used to process oxide semiconductors and gate dielectrics are spin-coating, inkjet printing and dip-coating. [3], [4], [6]

1.1 High-κ dielectrics

Once the scalability of the field effect transistors in integrated circuits is increasing, the thickness of gate dielectric SiO_2 is going down until the nanometre scale is reached. As a consequence, the leakage current of SiO_2 raises up drastically due to the tunnelling effect. Then, many researchers have been led to investigate ultrathin dielectric materials which have high permittivity, large capacitance, low leakage current density, thermal stability, amorphous structure and reliability.[6]–[11] These characteristics allows low voltage operations as well the induction of large densities in the semiconductor.[3], [13], [14] Some of the most investigated high-κ inorganic dielectrics are hafnium oxide (HfO_2), lanthanum oxide (La_2O_3), Iridium oxide (Y_2O_3), zirconium oxide (ZrO_2) and aluminum oxide (Al_2O_3).[7], [15]

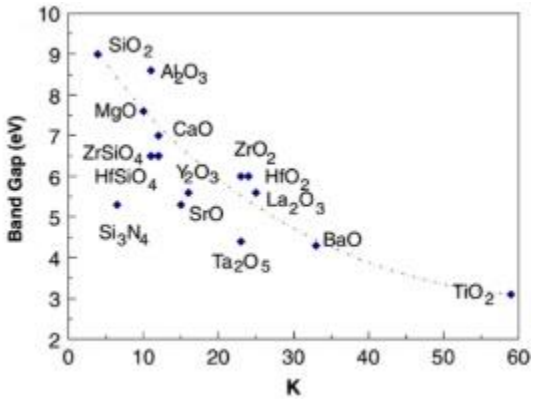

Figure 1.1 - Relation between the band gap and the static dielectric constant for different materials considered as high-k dielectrics.[15]

Despite many suitable dielectric materials to work as gate insulators, Al_2O_3 offers good properties such as large band gap (8.9 eV), high dielectric constant (~9), low interface trap density with semiconductors, large conduction band offset with silicon substrates (ΔE>3 eV), high breakdown electric field (4-5 MV/cm) and the capability of remaining amorphous in typical processing conditions. Furthermore Al_2O_3 is an amphoteric oxide with an high thermal conductivity (30 $Wm^{-1}K^{-1}$). [3], [10],[16]

1.2 Sustainable Production

Nowadays, 2-Methoxyethanol (2-ME) continues to be one of the most widely used organic solvent in the solution synthesis for the metal oxide thin films formation,[17] however it has some characteristics that disfavour the solvent, namely health hazardousness and harmfulness. Eco-friendly solvents allow the minimization of the environmental impact and facilitates their integration in large area production. Around the "green" solvents, four directions have been developed, such as the ionic liquids,[18] the substitution by supercritical fluids,[19], [20] the use of solvents produced with renewable resources and the substitution of hazardous solvents for ones which show better environmental, health and safety (EHS) properties. [21] The last direction taken was the one used in this work.

Some work starts to emerge few years ago focusing on "green" solvents, such as Branquinho *et al.* which reported amorphous AlO_x thin films developed by solution combustion synthesis (SCS) using for the first time environmental friendly water-based precursors. Nevertheless, high annealing temperatures were still necessary, to guarantee a degradation of the organic content.[22]

Also, the same group reported AlO_x made by SCS using for the first time ethanol as solvent and a maximum processing temperature of 350°C. [23] Recently, a more friendly solvent with similar properties to 2-ME (boiling point, polymeric chain size), 1-methoxy-2-propanol (1-MP) was tested to produce low ZrO_x dielectrics at low temperature. [24]

1.3 Low thermal budget techniques to process metal oxides

Solution-based amorphous metal oxides are reaching a similar properties to oxide semiconductor films grown by physical vapour deposition (PVD).

However, the solution-based method requires a high expense of energy due to an annealing step at high temperatures necessary to process the film, which is incompatible with flexible low cost substrates. [1], [3], [5], [20], [22]

To solve the previous problem, researchers tried a new approach with the purpose of reducing the temperature required to produce solution-processed metal oxide thin films by using a self-energy generating combustion chemistry method. With this solution becomes possible the fabrication of high-performance thin film transistors (TFTs) on flexible substrates.[3], [5] The technique is designated by solution combustion synthesis (SCS). SCS is a popular method for the preparation of a wide variety of materials owing to its simplicity, broad range of applicability and the possibility of easily obtaining products in the desired composition. This method has been broadly used to develop oxide powder and thin film materials, thus is becoming one of the most convenient processes of oxides preparation for electronic applications. [5], [26]–[28] Solution combustion synthesis is based on a redox system constituted by the nitrate ions gathered from the metal precursor, acting as oxidizer, and a fuel, such as urea, glycine or citric acid, which after heated up to moderate temperatures, occurs a strong exothermic redox reaction.[26], [29] Figure 1.2 shows a schematic of MO film synthesis via self-combustion of aluminum precursors bearing coordinated fuel and oxidizer ligands.

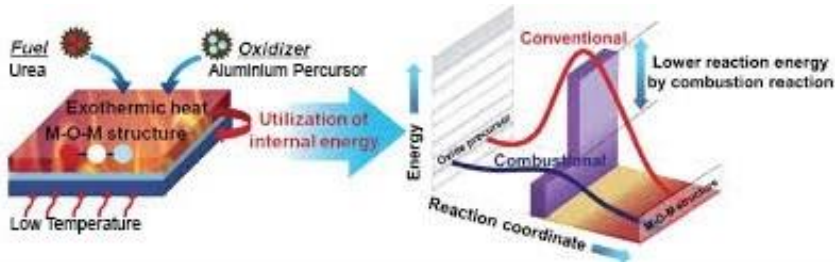

Figure 1.2 – A schematic diagram of MO film synthesis via self-combustion of aluminum precursors bearing coordinated fuel and oxidizer ligands. [66]

Another method to reach high-performance and stable metal-oxide semiconductors at low temperature is deep-ultraviolet (DUV) irradiation. This technique combined with thermal annealing improves the condensation and film densification maintaining the amorphous phase of the thin films. [1], [30] The solution-based amorphous metal oxides thin films need the DUV treatment (the main peaks of the UV lamp at 184.9 nm (10%) and 253.7 nm (90%)) to remove the residual organic components under a nitrogen atmosphere. The high-energy DUV photons induce photochemical cleavage of alkoxy groups and activate metal and oxygen atoms to convert easier the metal-oxide-metal (M-O-M) network formation. The UV irradiation can break the polymeric chains into smaller molecules causing a fast degradation, removal of oxygen and carbon that promotes the film densification. [2], [16], [21], [22]

There is another technique identical to DUV, denominated far ultraviolet irradiation (FUV), however uses a shorter UV wavelength (160 nm). The FUV irradiation combined with thermal annealing at low temperatures, also accelerates the condensation process leading to a rapid formation of the metal-oxide-metal structure, which makes it compactible with flexible substrates. Moreover, with this irradiation lamp it is possible to use a short processing time making it more suitable in R2R manufacturing. [3], [31], [32]

1.4 Thin Film Capacitors

Capacitors are part of electronic circuits used to store electric power by accumulating electrical charges in unbalanced levels. There are different types, shapes and sizes of capacitors, however the common structure consists in two conductor plates, which transport equal but opposite charges (+q and -q) with an insulator between them with a thickness (d). [3], [27], [33] The charge is obtained by the potential difference (V) between the plates and by the capacitance (C):

$$q = CV \tag{1}$$

The capacitance, measured in Farads (F), of any capacitor with parallel plates depends of some parameters, such as the plate area (A), the dielectric's thickness (d), the dielectric constant of the insulating material (κ) and the vacuum permittivity (ε_0). So, capacitance depends on the geometry and size of the plates but does not depend on the potential difference.[3], [27], [33]

$$C = \kappa \varepsilon_0 \frac{A}{d} \tag{2}$$

In the case of the Metal-Insulator-Semiconductor (MIS) capacitors, the capacitance changes according to the applied voltage derived from the presence of a semiconductor, for instance silicon. To reach the capacitance value in MIS capacitors, it is necessary to characterise the structures using capacitance-voltage (CV) curves and involves an applied bias voltage at the capacitor terminals. The voltage applied is split between the semiconductor and the insulating oxide, so according to that, the total capacitance (C_t) of the MIS structure is equal to the capacitance of the oxide (C_{ox}) plus the capacitance of semiconductor depletion-layer (C_D) associated in series correspond to: [3], [27], [34], [35]

$$\frac{1}{C_t} = \frac{1}{C_{ox}} + \frac{1}{C_D} \tag{3}$$

There are three operating domains when is applied a voltage sweep in the capacitor (I) the accumulation, (II) the depletion and (III) the inversion. The operation domains are shown in figure 1.3 (b).

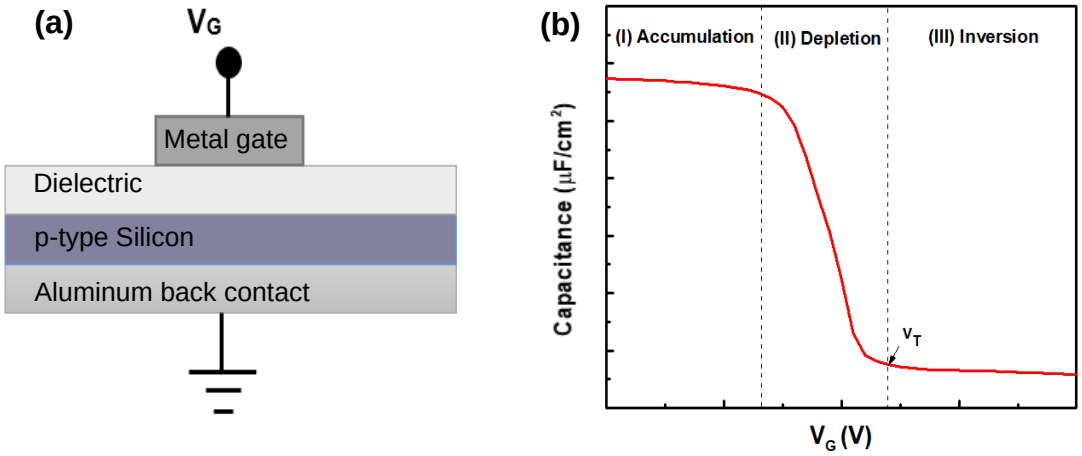

Figure 1.3 - (a) Metal-Insulator-Semiconductor structure schematic; (b) Typical Capacitance-Voltage curve of a p-type silicon semiconductor based MIS structure

(I) Accumulation: Without voltage being applied, a p-type semiconductor has holes, the majority carriers, in the valence band. When the MIS structure have a negative voltage (V_G) applied between the top contact (metal gate) and the semiconductor, more holes will appear in the valence band at the oxide-semiconductor interface. This happens once the negative charge of the metal causes an equal net positive charge to accumulate at the oxide-semiconductor interface. This domain of the p-type semiconductor is denominated accumulation. At that point, for a p-type MIS capacitor, the total capacitance (C_t) in this region is obtained by the insulator (dielectric) capacitance (C_{ox}), because the capacitor acts as one parallel plate capacitor. [3], [27], [34], [36], [37]

(II) Depletion: After accumulation, the majority carriers are repelled from the semiconductor-oxide interface, when a positive voltage (V_G) is applied between the gate and the semiconductor. This zone of the semiconductor is denominated depletion because of the depletion of majority carriers in the surface of the semiconductor. This area of semiconductor works as a dielectric once it can no longer contain or conduct charges. The total capacitance (C_t) measured is now equal to the oxide capacitance (C_{ox}) and the depletion layer capacitance (C_D) in series, so, the measured capacitance will decrease. [3], [27], [34], [36], [37]

(III) Inversion: As gate voltage (V_G) of a p-type MIS capacitor overcome the threshold voltage (V_T), the region of the depletion achieves the maximum depth and further gate-voltage increases and stop the depletion in the semiconductor. The positive gate voltage attracts electrons up to the gate. These electrons (minority carriers) accumulate at the semiconductor-oxide interface. The layer created by the electrons is called inversion layer since the carrier polarity inverts. When the depletion region reaches maximum depth, the total capacitance (C_T) is measured by the oxide capacitance (C_{ox}) in series with the maximum depletion capacitance (C_D). In a CV curve, this region is referred as minimum capacitance. [3], [27], [34], [37]

On the other hand, Metal-Insulator-Metal (MIM) capacitors are produced on flexible substrates, such as Kapton. This polyimide substrate is a common polymer used in the flexible electronic devices as a substrate. In this work, Kapton was chosen due to its high thermal stability (up to 400 °C), great dielectric properties and even high chemical resistance to acetone and isopropyl alcohol.[38][39]

Relatively to the Metal-Insulator-Metal (MIM) capacitors, they are pointed as next-generation capacitor due to its highly conductive electrodes and low parasitic capacitance. Even so, the absence of the depletion zone in these structures provide improved voltage linearity. [40]–[42] In figure 1.4 are presented the MIM schematic and the operation domains.

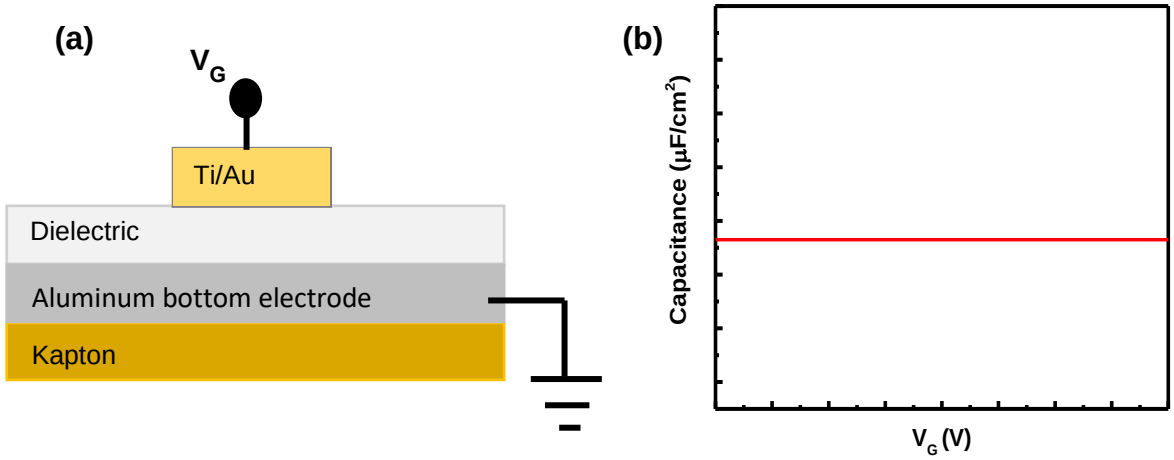

Figure 1.4 - (a) Metal-Insulator-Metal structure schematic; (b) Typical Capacitance-Voltage curve of a Kapton based MIM structure.

1.5 Evolution of Solution-based Thin Film Transistors

In the last years, amorphous oxide semiconductors based thin film transistors (TFTs) are referred to be the most suitable devices for the nearly future generation displays, like flexible and transparent devices, because they show great electrical performances such as high electron mobility and transparency.[23], [43], [44] However, these high performance oxide TFTs normally require physical vapour deposition (PVD) techniques, which are vacuum-based, resulting in high cost techniques, being a huge drawback when tried to produce TFTs in large-area devices.[5], [45] With the evolution of the solution-based oxide TFTs, these started to be compared to PVD-derived devices.[9], [46] However, to reach solution-based oxide TFTs on flexible substrates, it is necessary a reduction of the temperature fabrication process.[43], [45]

Despite the existing metal oxide semiconductors, indium oxide (In_2O_3) has been widely used due to is high electron mobility and its high optical transparency in visible region. This semiconductor can be achieved by solution processes and shows good electrical properties characteristics. So, solution-based indium oxide has been chosen as the semiconductor to be combined with solution-based Al_2O_3 to produce high performance oxide TFTs at low temperature. [45], [47]

2. Materials and Methods

Solution-based AlO_x thin film dielectrics were produced using different annealing conditions, molar concentrations and solvents. The optimization of these thin films was done through MIS capacitors. After the MIS structures were optimized, fabrication of MIM capacitors was performed on polyimide substrates. Finally, the application of the aluminum oxide thin films dielectrics on indium oxide TFTs was performed.

2.1 Precursor Solutions Preparation and Characterization

The precursor solution was prepared with aluminum nitrate nonahydrate ($Al(NO_3)_3 \cdot 9H_2O$, Fluka, 98%) dissolved in different solvents, 2-methoxyethanol (2-ME, $C_3H_8O_2$, Fisher Chemical, ≥ 99%), 1-methoxy-2-propanol (1-MP, $C_4H_{10}O_2$, Sigma-Aldrich, ≥ 99.5%) and Ethanol Absolut Anhydrous (C_2H_6O, CARLO ERBA, ≥ 99.5%), in concentrations of 0.1 M and 0.2 M. 1-Butanol (1-Bu, $C_4H_{10}O$, Panreac, ≥ 99%) and Millipore water (H_2O) were also used. To dissolve completely the solution should remain under constant stirring at 430 rpm for 15 minutes. To complete the combustion reaction precursor solutions, the fuel, urea ($CO(NH_2)_2$, Sigma-Aldrich, 98%) was added to the prepared solutions, which were maintained under constant stirring for at least 1 hour. To assure a redox stoichiometry of the reaction (Annex A) a molar proportion of 2.5:1 was established between the urea ($CO(NH_2)_2$, Sigma, 98%) and aluminum nitrate precursor.

Aluminum nitrate precursor solutions prepared using 2-ME and 1-MP as solvents were placed in a ceramic crucible and submitted in an air furnace (Nabertherm) with an initial temperature of 20 °C and a heating ramp of 10 °C/min. When the temperature reaches the 300 °C, it stays there for 1 hour. The powders were removed from the crucibles with the help of a spatula and used for X-ray diffraction (XRD) measurements. These were performed by an X-Ray diffractometer (XRD, X'Pert PRO PANalytical) measured at 45 kV and 40 mA, between 2θ = 10 ° and 2θ = 90 ° with a step size of 0.05 ° and equipped with a Cu Kα source (λ = 1.540598 Å).

Thermal characterization of aluminum nitrate precursor solutions was performed by thermogravimetry and differential scanning calorimetry (TG-DSC). These precursor solutions, with 0.2 M, were submitted to a partial slow solvent evaporation, acquiring a higher viscosity. 2-ME and 1-MP precursor solutions were heated at 90 °C and ethanol precursor solution at 60 °C, remaining under stirring, with the open flask, at 300 rpm until reaching a good viscosity. TG-DSC analysis were performed under air atmosphere up to 550 °C with a 20 °C/min heating rate in an aluminum crucible with a punctured lid using a simultaneous thermal analyzer, Netzsch (TG-DSC - STA 449 F3 Jupiter).

The absorbance spectra of precursor solutions were obtained by Fourier-transform infrared spectroscopy (FTIR, NICOLET 6700) using attenuated total reflectance (ATR). Precursor solutions data were measured between 4500 to 525 cm^{-1} wavenumber.

The indium precursor solution was prepared with indium (III) nitrate hydrate ($In(NO_3)_3 \cdot xH_2O$, Sigma, 99.9%) dissolved in 2-methoxyethanol ($C_3H_8O_2$, Sigma, >99.5%) with 0.2 M. Urea ($CO(NH_2)_2$, Sigma, 98%) was added to the indium nitrate solution with a molar proportion of 2.5:1.

2.2 Thin Film Deposition and Characterization

Prior to deposition all substrates (silicon p-type, single crystal, 100-oriented silicon wafer, soda-lime glass and Kapton with an area of 2.5×2.5 cm^2) were cleaned in an ultrasonic bath at 60°C in acetone for 10 min, then 2-isopropanol (IPA) for 10 min, after that were submerged in Millipore water by 15 seconds and dried under N_2; followed by 15 min UV/Ozone surface activation step for a distance lamp of 5 cm using a PSD-UV Novascan system. The precursor solutions chosen had concentrations of 0.1 M and 0.2 M and were filtered by using a 0.45 µm polytetrafluoroethylene (PTFE) or Regenerated cellulose (RC) syringe filter. Thin films were deposited by spin coating for 35 s at 2000 rpm, using 1 layer for MIS capacitors and 2 layers for MIM capacitors. In MIS capacitors the annealing conditions

used were (i) annealing at 300°C on a hot plate for 30 min; (ii) annealing at 150°C assisted by DUV (PSD Pro Series – Digital UV Ozone System Novascan) kept at 2 cm from thin films for 30 min in N_2 condition and (iii) annealing at 150°C assisted on DUV (PSD Pro Series – Digital UV Ozone System Novascan) kept at 2 cm from thin films for 1 h in N_2 condition, while in MIM capacitors the (iii) annealing at 150°C assisted on DUV (PSD Pro Series – Digital UV Ozone System Novascan) kept at 2 cm from thin films for 1 h in N_2 condition per layer was the only used.

The absorbance spectra of thin films were measured using an ATR-FTIR (NICOLET 6700). Measurements were taken between 4500 to 525 cm^{-1} wavenumber.

To obtain the thin films optical properties a Perkin Elmer lambda 950 UV-Vis-NIR spectrophotometer was used. Thin films transmittance was taken in soda-lime glass substrates in a range between 200 to 800 nm wavelength.

The spectroscopic ellipsometry measurements provided the thickness of thin films deposited on silicon substrates, which were made over an energy range of 1.5−6.5 eV with an incident angle of 70° using a Jobin Yvon Uvisel system.

The thin films structure was obtained by glancing angle X-ray diffraction (GAXRD) performed by an X'Pert PRO PANalytical powder diffractometer between 2θ = 10 ° and 2θ = 60 ° with a step size of 0.2 ° using CU Kα line radiation (λ = 1.540598 Å) with X-ray beam incident angle fixed at 0.9 °.

To study the roughness of thin films deposited on the Kapton substrates resorted to an atomic force microscope (AFM, Asylum MFP3D). The scanning size used was 5×5 μm^2 and the RMS of Kapton surface achieved was 1.211 nm.

2.3 Electronic Device Fabrication and Characterization

2.3.1 MIS Structures

Firstly, to produce the metal-insulator-semiconductor (MIS) capacitors an aluminum oxide single layer was deposited by spin-coating in silicon substrates and followed by an: (i) annealing at 300°C on a hot plate for 30 min; (ii) annealing at 150°C assisted by DUV (PSD Pro Series – Digital UV Ozone System Novascan) kept at 2 cm from thin films for 30 min in N_2 condition and (iii) annealing at 150°C assisted on DUV (PSD Pro Series – Digital UV Ozone System Novascan) kept at 2 cm from thin films for 1 h in N_2 condition.
The schematic of MIS structures production is presented in Annex B.

MIS capacitors were produced by AlO_x thin film deposition onto p-type silicon substrates (resistivity between 1-2 Ω·cm) as previously described. Aluminum top electrodes (80 nm thick) with an area of 2×10^{-3} cm^2 were deposited by thermal evaporation via shadow mask.

An 80 nm thickness aluminum layer was also deposited by thermal evaporation on the back of the substrate to improve the ohmic contact. The electrical characterization was performed using a semiconductor parameter analyser (Keysight B1500A) with a probe station (Cascade EPS150 Triax) by measuring both the capacitance-voltage (CV) between -3.5 V and 1 V , capacitance-frequency (Cf) with V_{bias} = 3 V between 1 kHz and 1 MHz and current-voltage (IV) between -6 V and 1 V.

2.3.2 MIM Structures

For the production of metal-insulator-metal (MIM) capacitors two layers of the aluminum precursor solution were deposited by spin-coating on the top of Al bottom electrode, previously deposited by thermal evaporation. Both layers were subjected to an (iii) annealing at 150°C assisted by DUV irradiation (PSD Pro Series – Digital UV Ozone System Novascan) kept at 2 cm from thin films for 60 minutes. Between layers a UV/Ozone surface activation for at least 10 min was needed to guarantee

a good adhesion. To finalize these devices, a Ti/Au (6 nm and 60 nm, respectively) top electrode was deposited by e-beam evaporation, to distinguish the top contacts from the Al bottom layer. Summarizing, these devices presented an Au/Ti/AlO_x/Al structure on polyimide substrate.

The schematic of MIM structures is presented in Annex B.

For MIM capacitors, the CV curve range was -0.5 V to 0.5 V, for Cf curve V_{bias} = 0.1 V and for IV curve from 0 V to 6 V.

2.3.3 InO_x/AlO_x TFTs

To produce the thin film transistors (TFTs) two different annealing processes were performed. The aluminum oxide was deposited onto a silicon p-type, single crystal, 100-oriented silicon wafer as previously described and (i) annealed on a hot plate for 30 min at 300 °C. After the deposition of the dielectric it was deposited a single layer of the indium oxide precursor solution with the same annealing as aluminum oxide layer. After the layer deposition, it was submitted to a drying step of 130 °C for 15 min on a hot plate and then with the annealing at 300°C on a hot plate for 30 min. The same procedure was done for the (iv) annealing at 200°C combined with a short-wavelength far ultraviolet (FUV) photochemical activation. The lamp (H2D2 light source unit, model L11798) was located at a distance of 5 cm with a conventional thermo annealing for 30 min in N_2 condition.

To finalize InO_x/AlO_x TFTs were produced. After deposition and annealing of dielectric and semiconductor layers, an 80 nm thick Al source/drain (S/D) electrodes were deposited by thermal evaporation on the active layer through a shadow mask to obtain a channel width (W) of 1400 µm and a channel length (L) 100 µm. On the back of the substrate was also deposited an 80 nm thickness layer of Al using the thermal evaporator.

3. Results and Discussion

The results obtained for the precursor solutions characterization, thin films characterization and electrical characterization of MIS/MIM capacitors and TFTs are presented and analysed in the following chapter.

3.1 Precursor Solution and Powder Characterization

3.1.1 TG-DSC Analysis

Thermal analysis was realized to study the decomposition behaviour of the aluminium oxide precursors. In the figure 3.1 is shown the differential scanning calorimetry (DSC) and thermogravimetry (TG), results for aluminum nitrate nonahydrate ($(Al(NO_3)_3 \cdot 9H_2O)$) dissolved in 2-Methoxyethanol (2-ME), 1-Methoxy-2-propanol (1-MP) and ethanol absolute, using urea as fuel. Before using TG-DSC, the AlO_x xerogels were obtained from a slow evaporation using the respective solvents, to increase the ratio AlO_x / inorganic.

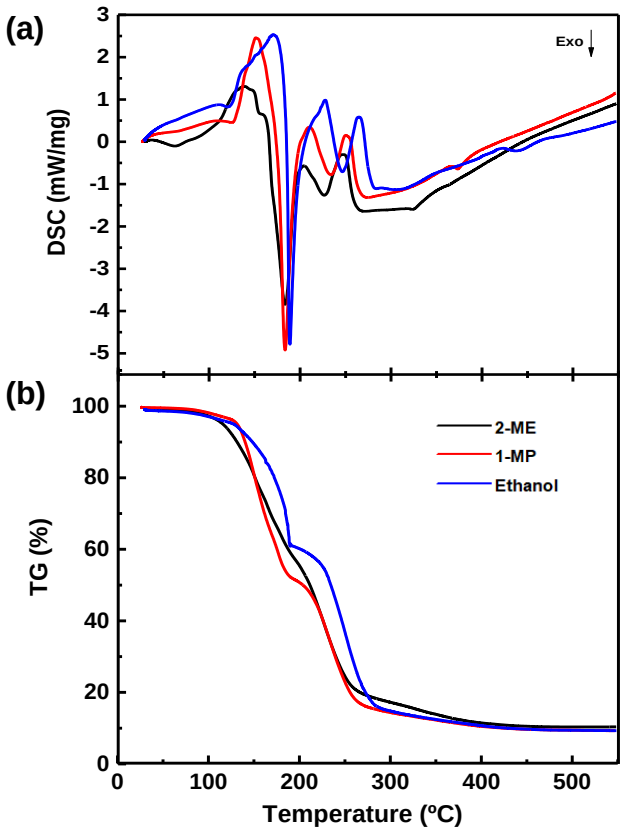

Figure 3.1 – (a) DSC analysis and (b) TG analysis of the aluminum nitrate solutions with 2-ME, 1-MP and ethanol as solvents with a C = 0.2 M.

In the figure 3.1, it is possible to observe intense exothermic peaks at the temperature of 183 °C for 2-ME and 1-MP, and at 188.6 °C for ethanol, temperatures which indicate the ignition of the combustion reaction. A smaller endothermic peak at 247 °C, 251 °C and 265 °C, respectively, attributed to the degradation of residual organics.

In differential scanning calorimetry graphic, the exothermic peaks correspond to a drastically mass loss in the thermogravimetry graphic (~40%).

Precursor solution thermal analysis confirm that the minimum temperature for full degradation of all aluminum nitrate precursor solution is 265 °C. Branquinho *et al.* reported a DSC-TG analysis of AlO_x precursor solutions using 2-ME and ethanol as solvents and urea as fuel, achieving the degradation temperature at 250 °C. [28]

3.1.2 Powder Characterization

The Alumina (AlO_x) powders were produced using a conventional oven for the aluminum precursor solution with different solvents, 2-methoxyethanol and 1-methoxy-2-propanol. To study the crystallinity of the AlO_x powders, XRD was obtained as depicted in Figure 3.2.

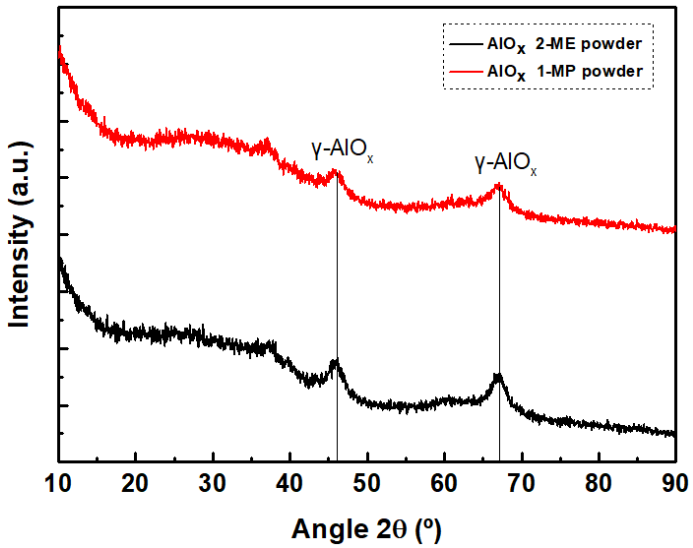

Figure 3.2 - Amorphous AlO_x powders with 2-ME and 1-MP as solvents with a C = 0.2 M.

Alumina presents different metastable structures, such as gamma (γ), theta (θ) or alpha (α). The most stable phase of alumina is alpha (α-AlO_X). [48] These crystalline phases emerged depending on the synthesis temperature and time of the reaction. The γ-AlO_x can appear from 200 °C, while the α-AlO_X can emerge from 1100 °C. [49] In figure 3.2 are observed two crystalline peaks (46 ° and 67 °) on 2-ME and 1-MP powders. Once these powders were synthetized at temperatures until 300 °C, it was expected alumina remains amorphous. However, the diffraction peaks presented, correspond to the alumina gamma phase (γ-AlO_X) [48] revealing crystallinity. These peaks can appear in powders due to the low crystallinity of powders.

3.2 Thin Films Characterization

After the thermal analysis of the solution, it is important to characterize the thin film optical properties and structure.

3.2.1 Structural Characterization

The solution-based AlO_x thin films assume different structures according to different annealing temperatures. Over 500 °C, these thin films change from amorphous and start to present a polycrystalline structure.[50] When the dielectric thin films change to a polycrystalline structure, more grain boundaries appear acting as high-leakage paths. On the other hand, amorphous thin films effectively prevent leakage current arising, providing isotropic electrical properties since no grain boundaries are present in the film. These films present a smoother surface and more uniform, which improves interface properties. [3], [12], [51]

The alumina thin films were analysed by X-ray diffraction. The technique was executed in the grazing angle mode for the thin film annealed at the highest temperature used (300 °C). These two diffraction peaks that appear in figure 3.3 are due to the silicon wafer (100) oriented used as substrate. The first peak emerges when 2θ = 51.7 ° and the second one at 2θ = 53.9 ° followed by a hump. These peaks coincide with the silicon wafer (100) oriented and appear when the grazing angle mode is used at a specific phi angle. [52] So it can be concluded that aluminum thin films are amorphous.

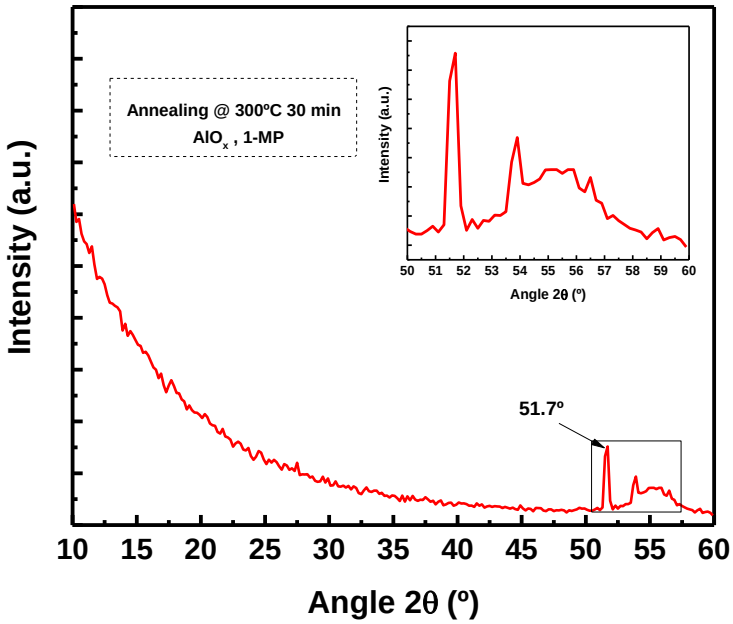

Figure 3.3 – Glancing angle X-ray diffraction (GAXRD) analysis of the AlO_x thin film annealed at 300 °C for 30 minutes using 1-MP as solvent

Both alumina powders (sub-section 3.1.2) and thin films were analysed by XRD. Although, powders presented a crystalline structure, while the alumina thin films remained amorphous, verifying only a peak, followed by a hump, owing to the silicon wafer (100) oriented.

3.2.2 Fourier Transform Infrared Spectroscopy (FTIR)

The AlO_x thin films were measured using FTIR, to identify which elements are presented in thin films through the obtained spectrum. To have the whole spectra for the different annealing conditions, the solutions were deposited in silicon substrates and the measurements were executed using

attenuated total reflectance (ATR). Figure 3.4 show the spectra absorbance in a range between 1200-550 cm^{-1} for the different annealing conditions and 2-ME solution.

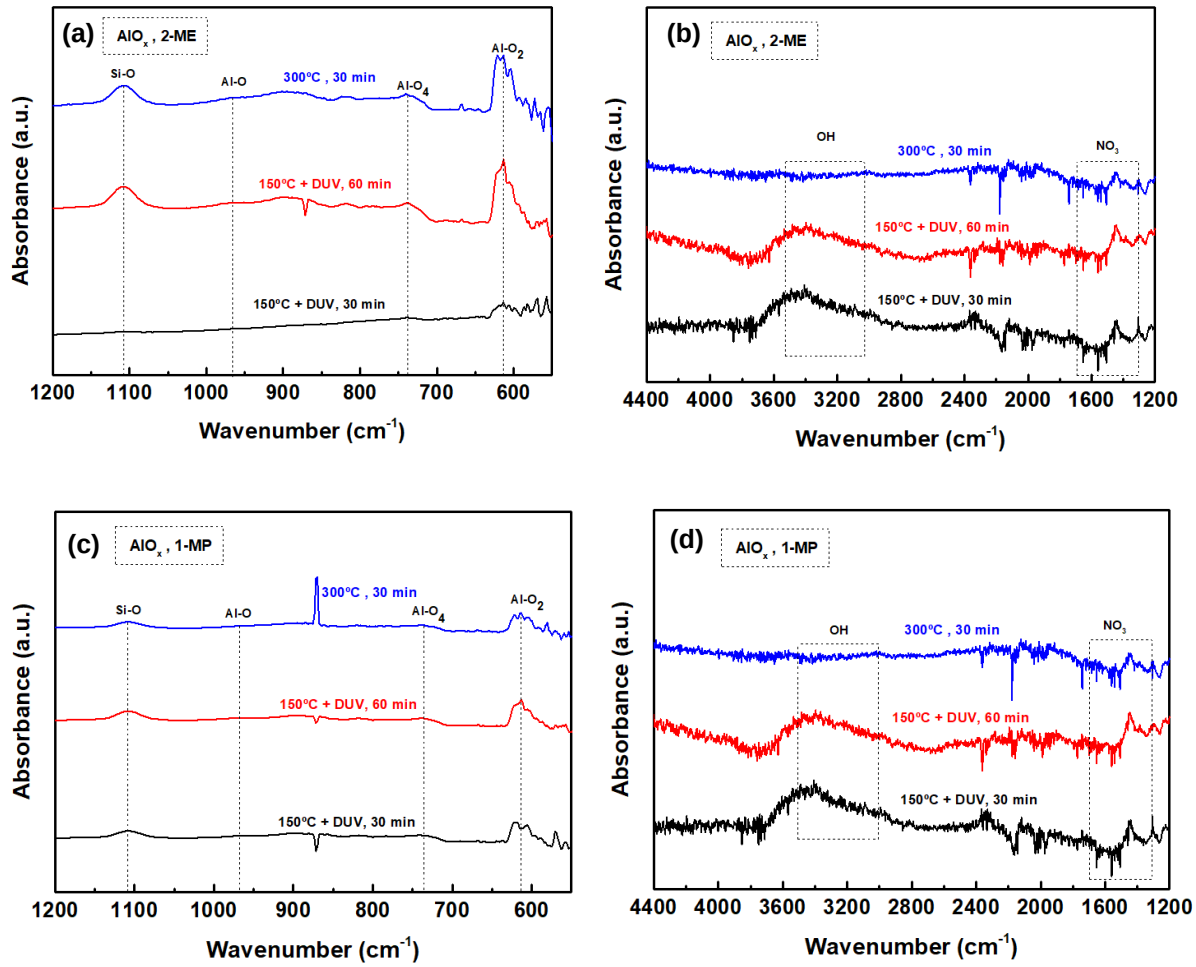

Figure 3.4 - FTIR-ATR analysis of AlO_x thin films with (a) 2-ME as solvent and C = 0.2 M, measured between 1200 to 550 cm^{-1} and (b) measured between 4400 to 1200 cm^{-1} and (c) 1-MP as solvent and C = 0.2 M, measured between 1200 to 550 cm^{-1} and (d) measured between 4400 to 1200 cm^{-1}.

Figure 3.4 (a) and (c) allows to identify some relevant absorbance peaks on AlO_x thin films. Alumina demonstrates different vibrational modes at 611, 739 and 968 cm^{-1} and Si-O vibration occurs at 1107 cm^{-1}.[3], [53]

Figure 3.4 (b) and (d) presents the spectra from the different annealing conditions and 2-ME solution, in a range comprehended between 4400-1200 cm^{-1}. It is observable between 3500-3000 cm^{-1} the presence of hydroxyl groups (OH) for 150 °C assisted by DUV annealing conditions. The presence of nitrate (NO_3) group deformation vibrations indicated by the peaks between 1700-1300 cm^{-1}. It is noticed the NO_3 groups show less intensity for temperatures equal to 300 °C or above, once these are gradually decomposing with the temperature increasing.[46]

3.2.3 Transmittance

The transmittance curves were obtained by a wavelength spectrum comprised between 200 and 800 nm with a wavelength step of 2 nm, for three different solutions deposited by spin-coating on soda-lime glass. All solutions have the same precursor (aluminum nitrate nonahydrate), same

concentration (0.2 M) and urea as fuel. The only change factor is the solvent used (2-ME, 1-MP or Ethanol). The thin films were produced using different annealing parameters. The respective measures are presented in figure 3.5 (a) for 2-ME, (b) for 1-MP and (c) for ethanol.

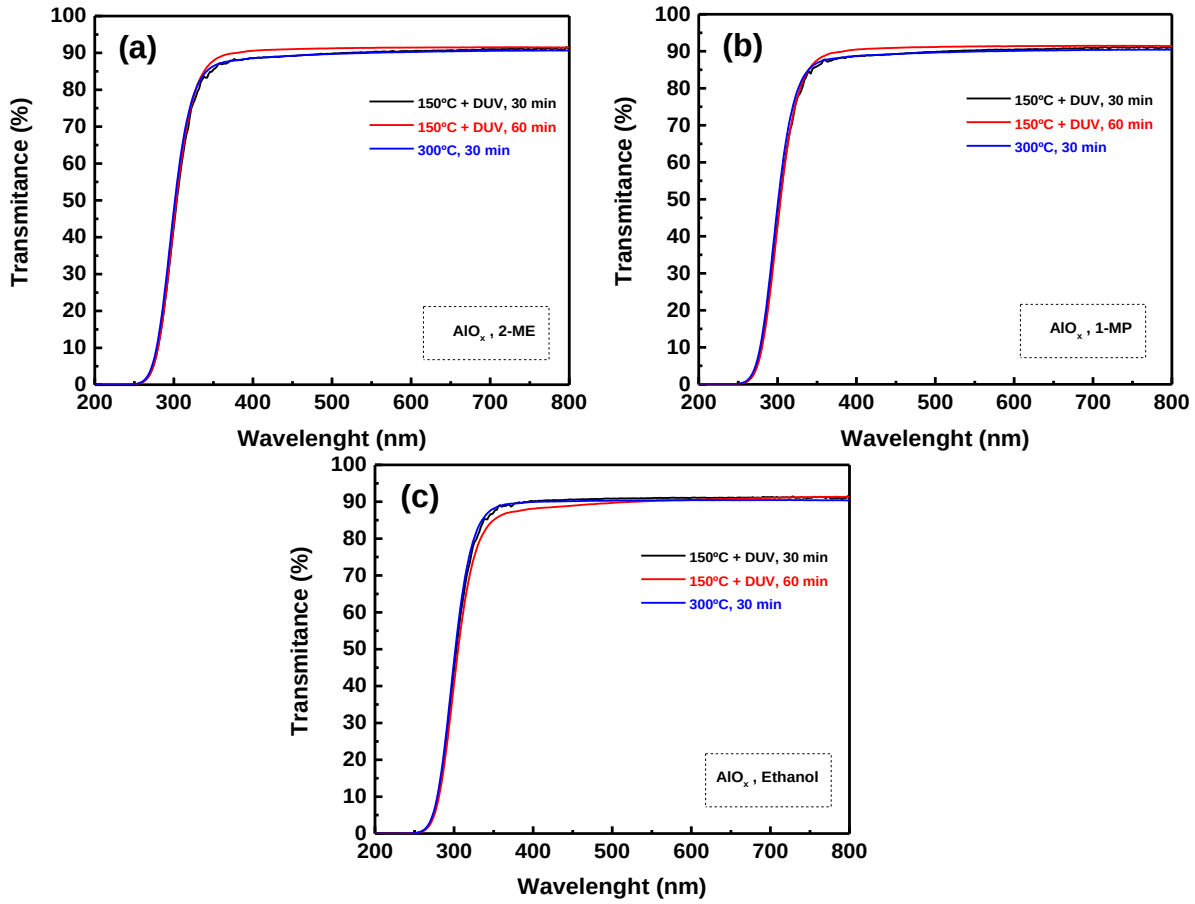

Figure 3.5 - Transmittance spectra of AlO_x thin films developed using (a) 2-ME, (b) 1-MP and (c) Ethanol as solvents in the synthesis and different annealing conditions.

By analysing figure 3.5, it is possible to verify, in the range of visible region (400-800nm), transmittances between 88% and 91%, regardless the solvent or annealing parameters used.

3.2.4 Thickness

To characterize the thickness of the thin films, spectroscopic ellipsometry was used, due to the small thickness of the thin films (less than 50 nm). In order to understand how thickness changes, the measurements were made for different processing parameters (solvents, concentration and annealing conditions) of the thin films. In the figure 3.6 below, the thin films analysed were produced with a concentration of 0.2 M concentration.

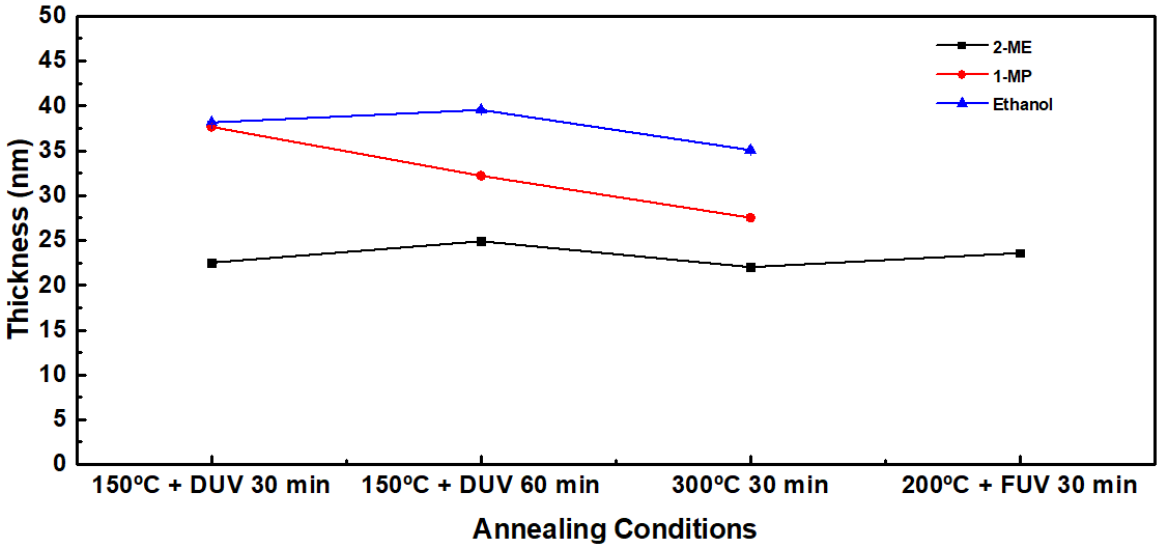

Figure 3.6 – Thickness of AlO_x thin films developed with 0.2 M solutions using 1 layer, different solvents and annealing conditions. The lines are guide for eyes.

In the figure 3.6 , it is possible to observe that either 1-MP and Ethanol are solvents that contributes for thin films with higher thickness than 2-ME, for all investigated conditions. To comprehend these differences, it was used a viscosimeter, however due to the lack of resolution of the equipment, it was not possible to measure the viscosity of the solutions, whereby a higher viscosity results in a thicker film. Nevertheless, the safety datasheet of 2-ME, 1-MP and ethanol presented dynamic viscosities of 1.7, 1.8 and 1.2 cP at 20 °C, respectively, with ethanol exhibiting an opposite behaviour.[54]–[56] The table 3.1 summarizes the thickness of 0.2 M concentration thin films with 1 layer.

Table 3.1 - Thickness of AlO_x Thin Films with 1 layer, C = 0.2 M

Annealing Conditions	Solvents	Concentration (M)	Thickness (nm)
150 °C + DUV for 30 min	2-ME	0.2	24.5 ± 0.07
	1-MP		31.6 ± 0.07
	Ethanol		42.6 ± 0.18
150 °C + DUV for 60 min	2-ME		24.9 ± 0.09
	1-MP		32.2 ± 0.07
	Ethanol		39.5 ± 0.15
300 °C for 30 min	2-ME		25.3 ± 0.09
	1-MP		27.5 ± 0.12
	Ethanol		35.1 ± 0.12
200 °C + FUV for 30 min	2-ME		23.6 ± 0.04

The table 3.2 shows the thickness results for AlO_x thin films obtained with 1 layer and 0.1 M concentration.

Table 3.2 - Thickness of AlO_x Thin Films with 1 layer, C = 0.1 M

Annealing Conditions	Solvents	Concentration (M)	Thickness (nm)
150 °C + DUV for 30 min	2-ME	0.1	12.7 ± 0.10
	1-MP		14.3 ± 0.07
300 °C for 30 min	2-ME		15.5 ± 0.37
	1-MP		14.0 ± 0.07

Comparing the results obtained in table 3.2, the thin films with different solvents have similar behaviours over the annealing conditions measured. While the thickness of 2-ME thin films have a low increase from 12.7 ± 0.1 nm (150 °C assisted by DUV for 30 minutes) to 15.5 ± 0.4 nm (300 °C for 30 minutes), the 1-MP thin films keep a similar thickness (14.3 ± 0.1 nm and 14 ± 0.1 nm, respectively).

The thickness of thin films with 2-ME as solvent and two layers with 0.2 M concentration using 150 °C assisted on DUV for 60 minutes per layer deposited on the silicon wafer (100 oriented) was measured. The thickness obtained for this thin film is presented in table 3.3.

Table 3.3 - Thickness of AlO_x Thin Films with 2 layers, C = 0.2 M

Annealing Conditions	Solvents	Concentration (M)	Thickness (nm)
150 °C + DUV for 60 min	2-ME	0.2	42.6 ± 0.13

Comparing this value with the thin film using the same annealing conditions, although only with 1 layer (figure 3.6), it is observed the film with two layers has lower thickness.

Therefore, it is possible to conclude that higher solutions concentration, results in higher thin films thickness in the same annealing conditions. As for different solvents, ethanol-based thin films exhibit the higher thickness, while 2-ME-based thin films present the lower thickness. The thickness difference between these thin films is around 15 nm, showing a considerably difference. So, as lower the thickness of thin films, these should present higher capacitances as well as higher leakage currents.

3.3 Electrical Characterization of Solution-based Capacitors

The characteristics of insulating materials and the properties of insulator/semiconductor interface are highly related with the quality of thin film transistors (TFTs). To study the insulating layer, it was required metal-insulating-semiconductor (MIS) structures . The electrical characterization of the capacitors is focused on three different curves: capacitance-voltage (CV), capacitance-frequency (Cf) and current-voltage (IV). These curves enable to acquire important information about their performances, such as, the dielectric constant and the breakdown field of the dielectric layer.

In CV curves, the oxide capacitance (C_{ox}) is represented by the maximum capacitance measured in the accumulation zone. Capacitance-voltage curves exhibit hysteresis in a clockwise direction for all the different processing temperatures, which is justified by the charges trapping in the dielectric layer. [3] The Cf curves allow to understand the changes of the capacitance with the frequency (in a range between 1 kHz and 100 kHz) to different applied voltages in V_G. In I-V curves it is possible to determine the current behaviour when it passes through the device always considering the voltage applied on the gate. For a better comprehension of the data presented in the I-V curve, the current was divided by the electrode area and the applied voltage by the dielectric thickness, so the current density (J)-electric field (E) curve can be obtained. This JE curve allows to find which is the breakdown electric field and characterizing the current density of the devices.

The capacitors with a small area (≈0.2 mm^2) were selected, as smaller areas can minimize the probability of thin film defects during production, keeping a better uniformity.

In the next sections the values are shown considering at least 6 capacitors to show their variability.

The dielectrics capacitance is measured at a frequency of 1 kHz, since using lower frequencies could result in an exponential increase of the capacitance with the decrease of frequency due to low annealing temperatures. On the other hand, it allows to evaluate the solution-based thin film quality. This can be explained by the limited polarization response time. [2], [40]

3.3.1 Influence of the Solvents in AlO_x Thin Films

The first phase of this study involves testing different solvents which could substitute the 2-methoxyethanol (2-ME). To select the best solvents to work with, it was considered firstly the chemical similarity, safety and the environmentally friendliness. The tested solvents were 1-methoxy-2-propanol ($C_4H_{10}O_2$), ethanol absolute (C_2H_6O), 1-Butanol ($C_4H_{10}O$) and Millipore water (H_2O). All of the previous solvents are more eco-friendly than the 2-ME [57]. Some of the previous solvents did not allow to continue the capacitor fabrication. The aluminum oxide thin films using 1-Butanol (1-Bu) as a solvent, could not dissolve urea as a fuel, nevertheless it was tried the sol-gel reaction. However, after the annealing procedure the thin film shown a non-uniformity, as it can be observed in Annex C. It was also not possible to fabricate MIS capacitors using Millipore water as solvent owing to the lower thickness and existence of pinholes. In future, to increase thin film thickness, it could be deposited a second layer or produce a precursor solution with higher concentration.

The results obtained for the fabricated capacitors in standard conditions (300 °C for 30 minutes) with the different solvents are presented in the figure 3.7 below.

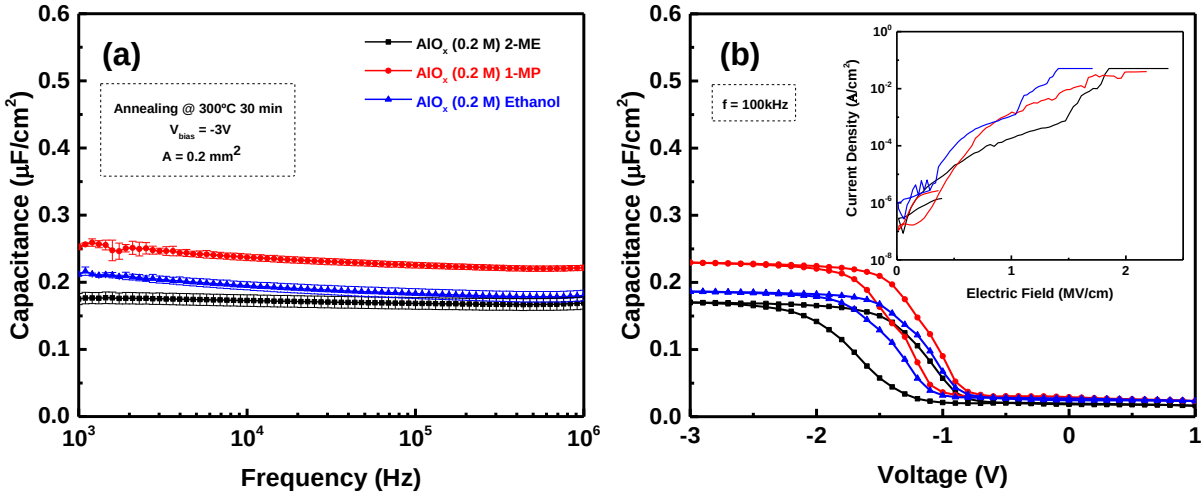

Figure 3.7 - Electrical characterization of solution-based AlO_x capacitors, with 0.2 mm^2 of area and 0.2 M, using 2-ME, 1-MP and ethanol as solvents at 300 ºC for 30 minutes. (a) Capacitance-frequency curve; (b) Capacitance-voltage curve taken at 100 kHz and on the inset current density-electric field curve.

In the figure 3.7 (a), capacitors produced with the 1-Methoxy-2-propanol as a solvent, show higher capacitance in a range between 1 kHz and 1 MHz, among the other developed devices, with 2-methoxyethanol and ethanol. This capacitance is due to the dielectric constant measured at 1 kHz (κ = 7.9) and the low thickness (27.5 nm). All the devices present a low capacitance variability with the frequency in the measured range. The figure 3.7 (b) compare the areal capacitance from the MIS structures with the applied voltage. The CV curve of all devices reveal some charges trapped in the dielectric layer, which can be indicated by the hysteresis. The high leakage current densities exhibited for AlO_x devices at 300 °C for 30 minutes (> 10^{-4} A/cm^2 at 1 MV/cm) is not ideal to TFT application.[58]

To evaluate the quality of the dielectric materials, it was calculated their dielectric constant (κ) using the equation (2) provided in sub chapter 1.4. The calculated permittivity for all cases were 5.0, 7.9 and 8.4 for 2-ME, 1-MP and ethanol respectively, thus the values were lower than expected for AlO_x (~9), however these results are in agreement with reported values for AlO_x solution-based. [6], [22], [23]

Table 3.4 – Electrical and physical properties of AlO_x thin film capacitors annealed at 300°C for 30 minutes.

Condition	Solvent	c (M)	C (nF/cm^2) at 1kHz	Thickness (nm)	κ at 1kHz	E (MV/cm)	J (A/cm^2) at 1MV/cm
300°C for 30 min	2-ME	0.2	175 ± 8	25.3 ± 0.09	5.0 ± 0.2	2.16 ± 0.02	(1.8 ± 2.0) x 10^{-4}
	1-MP		253 ± 4	27.5 ± 0.12	7.9 ± 0.1	1.99 ± 0.02	(1.5 ± 1.2) x 10^{-3}
	Ethanol		212 ± 2	35.1 ± 0.12	8.4 ± 0.1	1.46 ± 0.01	(1.2 ± 1.7) x 10^{-3}

Comparing the results in table 3.4, the capacitors with 1-MP presented higher capacitance at 1kHz, however present a higher leakage current. Although the ethanol-based AlO_x device exhibits a higher dielectric constant at 1 kHz, its breakdown electric field is the lowest among all, which means the device has poorer insulator properties. The capacitors produced with 2-ME shown lower leakage current and higher breakdown electric field, thus it makes the most stable device of the three.

3.3.2 Influence of the Annealing Temperature and DUV Treatment

The annealing step is essential to obtain high quality solution-based oxide dielectric devices. The annealing is important, because is where occurs the organic residues removal [59] and when is formed condensation and further densification of oxide layer. By submitting the thin films to different annealing temperatures with values ranging from 150 °C and 300 °C, it is possible to understand the relation between the annealing temperature and the electrical behaviour. To keep a good thin films quality by decreasing the annealing temperature, it is required perform annealing at 150°C under a deep-ultraviolet (DUV) treatment in a N_2 atmosphere.

The DUV treatment consists in a deep ultraviolet assisted photolysis, whose photons will provide an extra thermal energy in the annealing step. This DUV-assisted photolysis aids on the reorganisation of the M-O-M networks, without the need of high annealing temperatures.[1] The use of an DUV lamp in annealing process promotes the film densification by the formation of active oxygen species (O*). Since the as-fabricated solution-based M-O thin films contain significant amount of residual organic components, the active oxygen species are able to oxidize the organic ligands and the residual solvent transforming them into volatile gases using low temperature. By using this photoexcitation technique on the precursor, the decomposition from the organic groups occurs and metal-oxygen bonds emerge, turning the metal nitrate (precursor) into the metal oxide. [8], [60] The condensation/densification process is described in figure 3.8.

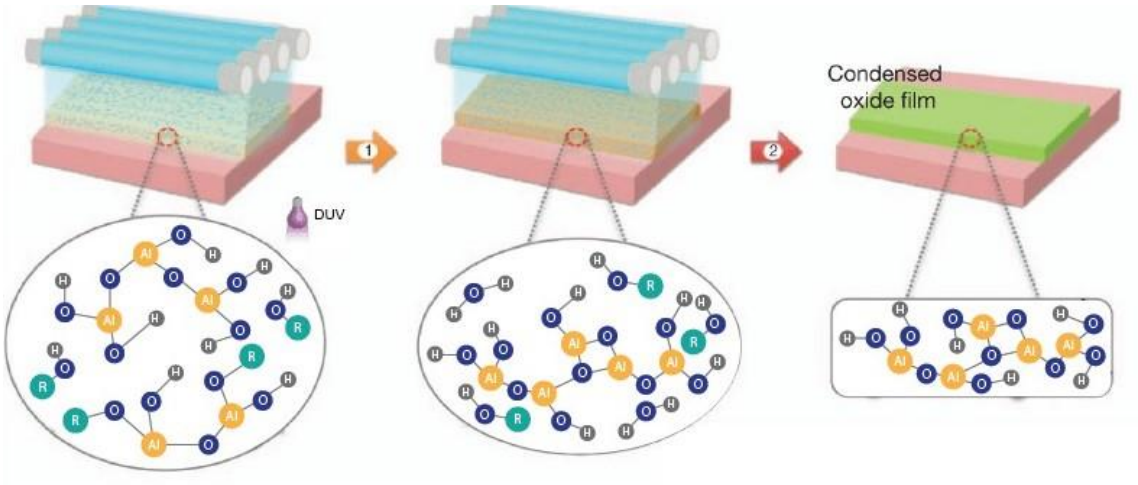

Figure 3.8 - Schemes showing condensation and densification mechanism of aluminum-oxide precursors by DUV irradiation. Light-blue shading denotes illumination from the low-pressure mercury lamp (blue cylinders).[1]

To analyse and compare the effect of annealing conditions it is necessary to characterize the electrical behaviour of the CV, Cf and JE curves. The figure 3.9 represents the plot of AlO_x capacitors for each solvent and with different annealing conditions.

In figure 3.9 (a), (c) and (e) is exhibited the Capacitance-frequency curve for the different annealing parameters and it is observed a general constant of areal capacitance with the increase of frequency is increasing, between a range of 10^3 Hz and 10^6 Hz. However, in (c) and (e), with the annealing temperature of 150 °C assisted by DUV for 60 minutes, the curves assume a decreasing trend. Xu *et al.* describes anomalous capacitances at annealing temperatures such 100 °C and 130 °C, as the existence of hydroxyl groups due to the low temperatures.[61] Nonetheless, since the 150 °C + DUV for 30 minutes condition demonstrate good stability as long is the frequency, it could be related to low polarization time.

Branquinho *et al.* demonstrates that the hysteresis of AlO_x thin films for lower temperatures than 350 °C, follows a decreasing trending line as low as the temperature, since the oxide charge defects associated with the dielectric, as a result of the incomplete organic residues removal.[28] Observing the CV curves on figure 3.9, the 150 °C + DUV annealing conditions presented similar hysteresis than the 300 °C for 30 minutes, denoting the 150 °C assisted by DUV for 60 minutes on 2-ME, which was obtained a significant lower hysteresis. Therefore, the exposure effect of ultraviolet irradiation increased the thin films quality at lower temperatures.

To investigate the leakage currents densities of the AlO_x (figure 3.9 (b), (d) and (f)), there are exhibited insets which show the behaviour of the current density with the electric field. The leakage currents obtained for the different annealing parameters were in a range between 10^{-2} and 10^{-7} A/cm^2 at 1 MV/cm. In this work, for capacitors with the 2-ME solution, the devices annealed at 300 °C have a leakage current of (1.8 ± 2.0) x 10^{-4} A/cm^2, while for the devices annealed at 150 °C with 30 and 60 minutes of DUV treatment have (2.1 ± 3.2) x 10^{-5} A/cm^2 and (2.1 ± 2.3) x 10^{-3} A/cm^2 respectively. Despite being expected the devices developed using DUV with further annealing time presented better electrical properties, it is not possible to establish a trend between the annealing parameters and the leakage current, however the devices worked successfully. To obtain thin films with the desirable dielectric properties, the combustion reaction of AlO_x has to occur above 187 °C for all the solutions, as demonstrated in DSC analysis (sub-section 3.1.1), which can justify the high leakage currents for 150°C annealed conditions, due to an inefficient organics removal. [28] The lowest leakage current was obtained for 1-MP at 150°C + DUV for 30 minutes is (8.4 ± 4.2) x 10^{-7} A/cm^2, which is significantly lower than the 300°C annealing conditions ((1.5 ± 1.2) x 10^{-3} A/cm). These results are very promising and demonstrate that the combination using low temperature and DUV treatment on this solution, creates a quality AlO_x thin films. Considering the annealing parameters for ethanol, the condition that exhibit the best behaviour is the temperature of 150 °C under DUV treatment for 30 minutes, which (1.1 ± 0.4) x 10^{-5} A/cm^2 leakage current. These results demonstrate good quality thin films at low temperature using eco-friendly solvents and they are suitable for use in gate dielectric for TFTs applications.

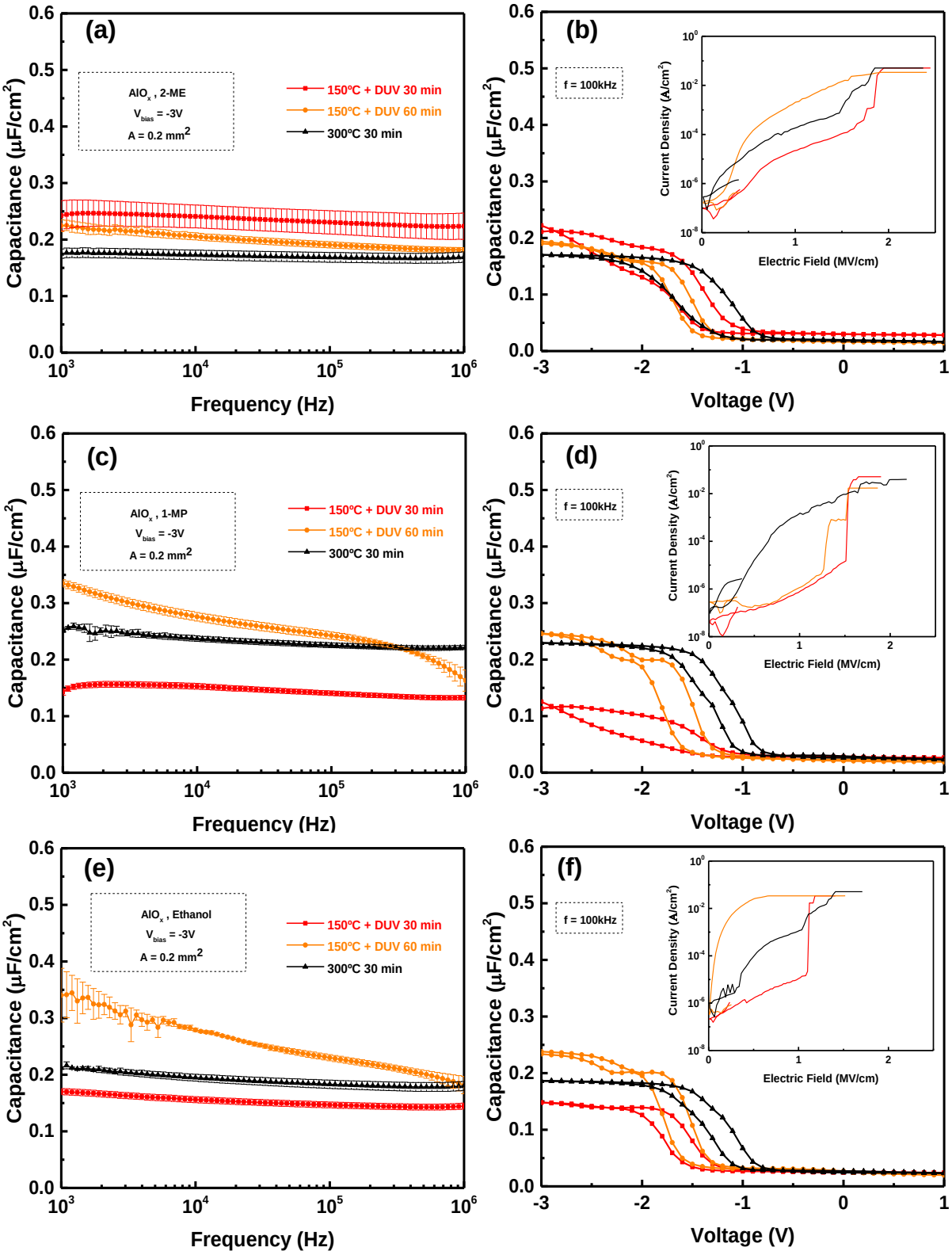

Figure 3.9 - Electrical characterization of AlO_x capacitors solution-based, with 0.2 mm^2 of area and 0.2 M, using different annealing conditions. (a) Cf curve for 2-ME; (b) CV curve for 2-ME at 100 kHz and JE curve on the inset; (c) Cf curve for 1-MP; (d) CV curve for 1-MP at 100 kHz and JE curve on the inset; (e) Cf curve for ethanol; (f) CV curve for ethanol at 100 kHz and JE curve on the inset.

For better comparation of AlO_x capacitors characteristics using different solvents and annealing conditions, table 3.5 presents a summary from the investigated data.

Table 3.5 - Summary of electrical and physical properties of AlO_x thin film capacitors with 0.2 M.

Condition	Solvent	c (M)	C (nF/cm^2) at 1kHz	Thickness (nm)	κ at 1kHz	E (MV/cm)	J (A/cm^2) at 1MV/cm
150°C + DUV for 30 min	2-ME	0.2	242 ± 27	24.5 ± 0.07	6.7 ± 0.7	1.95 ± 0.02	(2.1 ± 3.2) x 10^{-5}
	1-MP		143 ± 6	31.6 ± 0.07	5.1 ± 0.2	1.65 ± 0.01	(8.4 ± 4.2) x 10^{-7}
	Ethanol		170 ± 5	42.6 ± 0.18	8.2 ± 0.3	1.18 ± 0.01	(1.1 ± 0.4) x 10^{-5}
150°C + DUV for 60 min	2-ME		225 ± 11	24.9 ± 0.09	6.3 ± 0.3	1.99 ± 0.02	(2.1 ± 2.3) x 10^{-3}
	1-MP		335 ± 6	32.2 ± 0.07	12.1 ± 0.2	1.54 ± 0.01	(1.1 ± 0.9) x 10^{-6}
	Ethanol		340 ± 47	39.5 ± 0.15	15.2 ± 2.1	0.68 ± 0.01	(3.4 ± 2.4) x 10^{-2}
300°C for 30 min	2-ME		175 ± 8	25.3 ± 0.09	5.0 ± 0.2	2.16 ± 0.02	(1.8 ± 2.0) x 10^{-4}
	1-MP		253 ± 4	27.5 ± 0.12	7.9 ± 0.1	1.99 ± 0.02	(1.5 ± 1.2) x 10^{-3}
	Ethanol		212 ± 2	35.1 ± 0.12	8.4 ± 0.1	1.46 ± 0.01	(1.2 ± 1.7) x 10^{-3}

Summarizing, the capacitances obtained for 150 °C assisted with DUV for 60 minutes were generally higher than other annealing conditions (except for 2-ME). The dielectric constants measured at 1 kHz exhibited good values, [6], [23] except for 1-MP and ethanol annealed at 150 °C with DUV for 60 minutes, which were considerably higher. As for the leakage currents, the devices presented lower leak using as annealing temperature 150 °C assisted by DUV for 30 minutes.

Capacitors developed with 1-MP at 150 °C assisted by DUV for 60 minutes showed the most promising properties overall, as this condition presents low current density, high capacitance, high dielectric constant and it reveals environmental friendly, facing to the common option nowadays (2-ME).

3.3.3 Influence of the Solution Concentration in AlO_x Thin Films

To investigate the effect of the molar concentration in the MIS capacitors electrical performance, AlO_x thin films are prepared using 0.1 M and 0.2 M precursor concentrations dissolved in 2-ME and 1-MP. The solution with 0.1 M concentration dissolved in ethanol was not used since it acquired a blurred and whitish colour. The formation of hydroxyl groups in the solution can be responsible for this effect. Annex D demonstrate the solution obtained after stirred. The results are presented for the 2-ME devices annealed at 150°C with DUV for 30 minutes in figure 3.10.

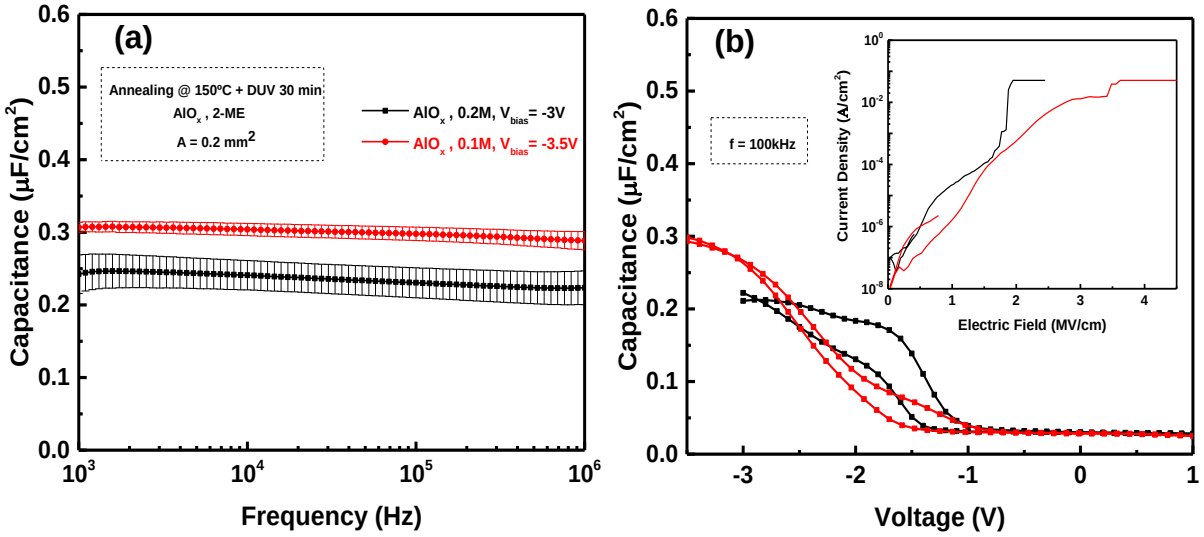

Figure 3.10 - Electrical characterization of AlO_x capacitors 2-ME solution-based, with 0.2 mm^2 of area and different concentrations (0.1 M and 0.2 M), annealed at 150 ºC assisted by DUV for 30 minutes. (a) Cf curve; (b) CV curve at 100 kHz and JE curve on the inset.

Table 3.6 summarizes the data presented on figure 3.10.

Table 3.6 - Electrical and physical properties of AlO_x thin film capacitors using 2-ME as solvent, annealed at 150 °C assisted by DUV for 30 minutes with 0.1 M and 0.2 M.

Condition	Solvent	c (M)	C (nF/cm^2) at 1kHz	Thickness (nm)	κ at 1kHz	E (MV/cm)	J (A/cm^2) at 1MV/cm
150°C + DUV for 30 min	2-ME	0.1	307 ± 7	12.7 ± 0.10	4.4 ± 0.1	3.62 ± 0.03	(1.7 ± 1.5) x 10^{-5}
		0.2	242 ± 27	24.5 ± 0.07	6.7 ± 0.7	1.95 ± 0.02	(2.1 ± 3.2) x 10^{-5}

The capacitance obtained for the device with 0.1 M precursor concentration is taken at a V_{bias} = - 3.5 V, to analyse the trend of the Cf curve, specifically, the accumulation zone. As expected, in figure 3.12 (a), the 0.1 M concentration capacitor presents a higher capacitance than the 0.2 M concentration capacitor, because thickness decreases as indicated in sub-section 1.4, equation (2). This shows how the capacitance varies theoretically. To obtain the desirable thin films, it is necessary to achieve the higher capacitance, trying to scale down the thickness (d) and preserving the dielectric properties.

In figure 3.10 (b), the CV curve for 0.1 M capacitor possess a significant lower hysteresis than the device developed with 0.2 M. As the concentration of the capacitor is increasing, the thin film becomes thinner and the ultraviolet irradiation does not work effectively, leading to a higher hysteresis.[3] On the inset, the 0.2 M capacitor presents higher leakage current due the increment of organic residues which were not degraded by DUV irradiation. The measurements in the 0.1 M capacitors exhibit some instability, because of the low dielectric constant.

In the figure 3.11 are presented the results for the 1-MP solution-based capacitor annealed at 150°C with DUV for 30 minutes.

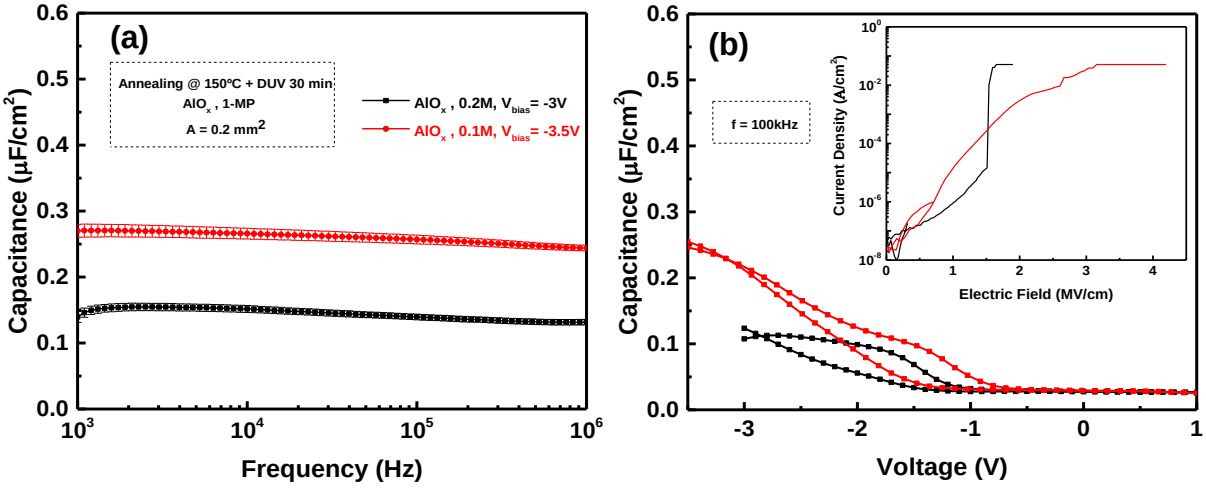

Figure 3.11 - Electrical characterization of AlO_x capacitors 1-MP solution-based, with 0.2 mm^2 of area and different concentrations (0.1 M and 0.2 M), annealed at 150 ºC assisted by DUV for 30 minutes. (a) Cf curve; (b) CV curve at 100 kHz and JE curve on the inset

Table 3.7 summarizes the data presented on figure 3.11.

Table 3.7 - Electrical and physical properties of AlOx thin film capacitors using 1-MP as solvent, annealed at 150 °C assisted by DUV for 30 minutes with 0.1 M and 0.2 M

Condition	Solvent	c (M)	C (nF/cm^2) at 1kHz	Thickness (nm)	κ at 1kHz	E (MV/cm)	J (A/cm^2) at 1MV/cm
150°C + DUV for 30 min	1-MP	0.1	270 ± 10	14.3 ± 0.07	4.4 ± 0.2	3.16 ± 0.03	(1.6 ± 2.3) x 10^{-5}
		0.2	143 ± 6	31.6 ± 0.07	5.1 ± 0.2	1.65 ± 0.01	(8.4 ± 4.2) x 10^{-7}

By analysing the figure 3.11 (a), it is possible to establish similarities with the capacitance voltage curve for the 2-ME capacitor. In spite of the capacitor behaviour maintains a practically constant capacitance over the frequency, this is lower than to the 2-ME device at the same conditions.

The CV curve, figure 3.11 (b), presents the same trend as the curve in figure 3.10 (b), however the hysteresis shown for 0.1 M device is slightly higher, which could be to the higher thickness of the 1-MP comparing with the 2-ME thin film. On the inset, at 1MV/cm, although the current density is higher on the 0.1 M capacitor, the breakdown electric field is also higher and it is equal to 3.16 MV/cm, when for the 0.2 M capacitor this occurs at 1.65 MV/cm. The unstable behaviour also occurs in the 0.1 M devices with 1-MP as solvent, such as 0.1 M capacitors developed with 2-ME as solvent.

To summarize, capacitors with 0.1 M concentration present better capacitance at 1 kHz and breakdown electric field than 0.2 M capacitors, while the last show higher dielectric constant at 1 kHz and thickness. The capacitor developed with 1-MP as a solvent with a 0.2 M concentration shows the lowest leakage current (8.4 ± 4.2) x 10^{-7} A/cm^2 at 1 MV/cm.

For future application in flexible substrates, the 0.2 M capacitors were chosen as their thickness ensure a quality dielectric layer on rougher surfaces and present higher dielectric constants. After

several developments, these flexible capacitors were selected to be used as gate dielectrics in a parallel work (as a proof of concept – section 3.4).

3.3.4 Flexible MIM AlO_x Capacitors

Since the AlO_x thin films exhibited a good electrical performance at low annealing temperatures (150 °C assisted by DUV), these were applied in flexible substrates. The application in flexible substrates leads to change on device structure from Metal-Insulator-Semiconductor (MIS) for Metal-Insulator-Metal (MIM). The polyimide substrate used has a rough surface, so were deposited two layers of AlO_x to cover the surface roughness of the substrate and avoid the short of the devices. To produce these dielectric thin films a thermal annealing at 150 °C assisted by DUV for 60 min per layer was performed. This annealing condition was chosen in order to be possible the application in Kapton, owing to low temperatures and because the thin films produced with showed a good electrical performance (sub-section 3.3.2). To test the influence of surface roughness of Kapton (polyimide substrate), atomic force microscopy (AFM) was used.

In this section, MIM AlO_x capacitors are developed using urea as fuel, 2-ME as solvent, 0.2 M concentration and depositing 2 layers.

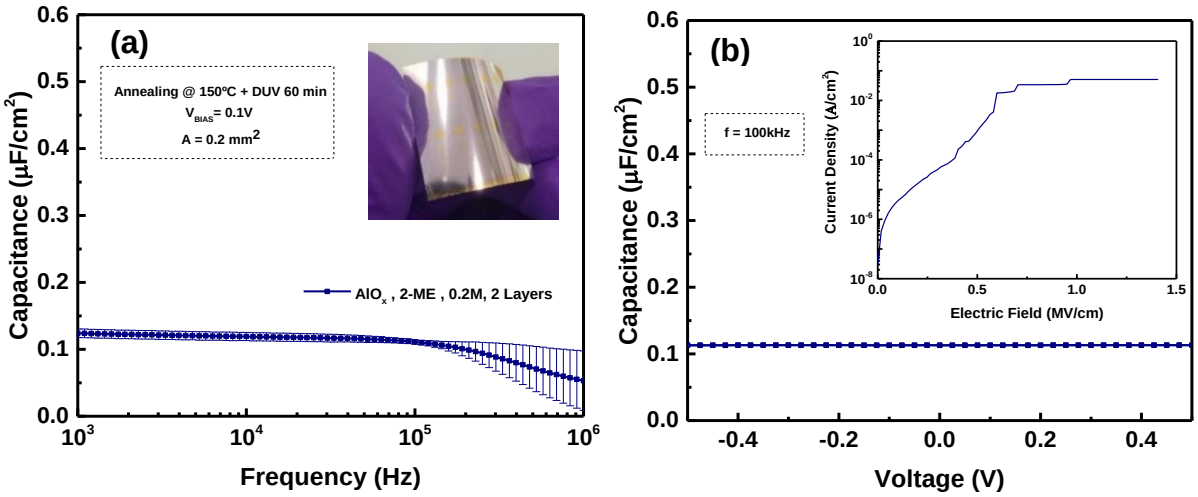

Figure 3.12 - Electrical characterization of solution-based AlO_x capacitors using 2-ME as solvent, with 0.2 mm^2 of area and 0.2 M, using 2 layers, annealed at 150 °C assisted by DUV for 60 minutes each. (a) Cf curve and a flexible prototype is on the inset; (b) CV curve at 100 kHz and JE curve on the inset.

In the figure 3.12 (a) is presented the capacitance-frequency curve and on the inset is showed a prototype of the flexible capacitors developed in this section, whereas in figure 3.12 (b) exhibits the capacitance-voltage curve and on the inset the current density-electric field curve.

The Cf curve demonstrate good stabilization of the frequency between the range of 1 to 100 kHz. Over in the range from 100 kHz until to 1 MHz, it is observed a decrease trend of the capacitance.

In the figure 3.12 (b), it is possible to observe that capacitance does not vary over the applied voltage, as expected, because of the absence of the semiconductor layer. This capacitor presents a leakage current of $(2.6 \pm 3.5) \times 10^{-5}$ A/cm^2 at 0.25 MV/cm, $(8.1 \pm 9.9) \times 10^{-4}$ A/cm^2 at 0.5 MV/cm and $(3.3 \pm 2.3) \times 10^{-2}$ A/cm^2 at 0.75 MV/cm, reaching the breakdown electric field at 0.97 MV/cm. Flexible devices have a higher tendency to present high leakage current and a small breakdown electric field, typically, because of the high roughness presented on the substrates (Annex F). Possible thin film cracks can contribute to higher leakage current and low breakdown electric field. [62] To patterning the devices could help to reduce leakage current as well as increasing the breakdown electric field.

Table 3.8 presents the summary of the flexible capacitors properties.

Table 3.8 - Electrical and physical properties of AlO_x thin film capacitors using 2-ME as solvent, with 0.2 M and 2 layers, annealed at 150 °C assisted by DUV for 60 minutes each.

Condition	Solvent	c (M)	C (nF/cm²) at 1kHz	Thickness (nm)	κ at 1kHz	E (MV/cm)	J (A/cm²) at 0.5 MV/cm
150 °C + DUV for 60 min (2 layers)	2-ME	0.2	124 ± 6	42.6 ± 0.1	6.0 ± 0.3	0.97 ± 0.01	(8.1 ± 9.9) x 10^{-4}

3.4 Electrical Characterization of Solution-based TFTs

This chapter exhibits the application of the most suitable dielectrics thin films for thin film transistors (TFTs) application, as proof of concept.

To develop these TFTs, the dielectric thin films applied on the TFTs were based in the 0.2 M aluminum nitrate solution with urea as fuel and 2-methoxyethanol as solvent. The solution-based semiconductor resorted was the indium oxide (In_2O_3) with a 0.2 M concentration. In the TFTs two different annealing conditions were used. Since the semiconductor thin films requires at least 200 °C as temperature to reach a proper conductivity and a quality film densification, the combination of 200 °C assisted with far ultraviolet irradiation (FUV) for 30 minutes and 300 °C for 30 minutes have been chosen.

The electrical performance of the AlO_x thin films with the annealing parameters used for the TFTs (200°C assisted by FUV for 30 minutes) are presented in Annex G. Thin films produced at 200 °C assisted by FUV for 30 minutes were successfully applied in solution-based TFTs. Figure 3.13 presents the In_2O_3/AlO_x TFTs transfer curves (I_{DS}-V_{GS}), using a drain voltage (V_{DS}) of 2 V and an applied gate voltage (V_{GS}) in a range of -1 V until 2 V.

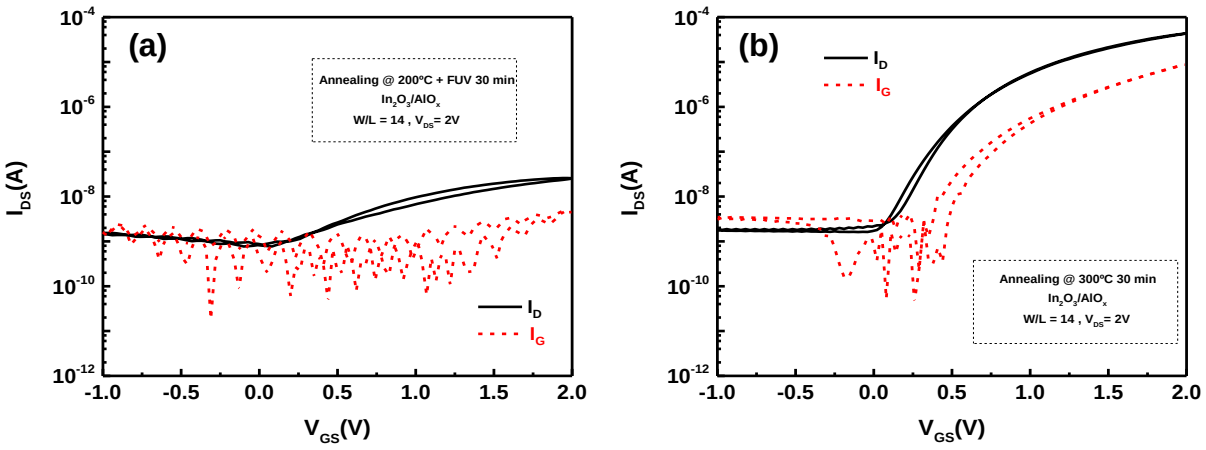

Figure 3.13 - In_2O_3/AlO_x TFTs transfer curves with an applied V_{DS} = 2 V and W/L = 14, (a) annealed at 200 ºC assisted by FUV for 30 min; (b) annealed at 300 ºC for 30 minutes.

Analysing the figure 3.13, the In_2O_3/AlO_x TFTs exhibit a relatively high gate leakage current, once the desired values should remain under 10^{-10} A. This happen, once the devices are not patterned.[63] The hysteresis in both TFTs are negligible. In_2O_3/AlO_x TFTs annealed at 300 °C exhibit lower subthreshold swing (SS) and higher I_{ON}/I_{OFF} ratio and saturation mobility (μ_{sat}), comparing with the devices annealed at 200 °C assisted by FUV. These results are summarized in table 3.9.

Table 3.9 – Summary electrical properties of In_2O_3/AlO_x TFTs

Condition	Capacitance (nF/cm^2) at 1kHz	W/L	I_{ON}/I_{OFF}	SS (V/decade)	V_T	μ_{sat} (cm^2/ Vs)
200°C + FUV, 30 min	247 ± 15	14	3.4×10^2	0.61	-0.09	0.0043
300°C, 30 min	175 ± 8		2.7×10^4	0.16	0.37	16.1

In the future, would be interesting to further develop In_2O_3/AlO_x TFTs using the alumina precursor solution for the fabrication of dielectric thin films, since it showed promising electrical performance.

4. Conclusions and Future Perspectives

Throughout this dissertation, all the work developed was focused on the optimization of AlO_x dielectric thin films by solution combustion synthesis, experimenting different eco-friendly solvents and low temperature annealing parameters, for application on flexible substrates. After achieving good quality AlO_x dielectrics, these were applied in TFTs.

After guaranteeing good characteristics on the precursor solutions by the thermal analysis, the resulting AlO_x thin films exhibited an amorphous structure, good transparency, and essential absorbance peaks.

The AlO_x thin films developed also presented good transmittance (> 85 %) and suitable thickness values.

Firstly, to characterize the electrical properties of the thin films was realised the measurement of at least 3 capacitors with an area of 0.2 mm^2. The solvents on the capacitors were selected using 300 °C for 30 minutes as annealing step, and devices presented good characteristics, namely 2-ME (standard), 1-MP and ethanol. The discarded solvents were Millipore water and 1-Butanol. Millipore water devices presented low thickness and existence of pinholes, whilst 1-Butanol could not dissolve using urea as a fuel and by sol-gel reaction the thin film demonstrate huge defects (Annex C). It is noteworthy the promising obtained capacitance from 1-MP capacitors.

Low temperature annealing, 150 °C assisted by DUV for 30 minutes, revealed a good behaviour on the capacitance over the frequency range measured. Despite the 150 °C assisted by DUV for 60 minutes worked well at 2-ME capacitors, on the 1-MP and ethanol devices, the capacitance assumes a decrease trend, most probably by the overexposure of the ultraviolet irradiation. The capacitance-voltage curve demonstrates a clear effect from the DUV on the hysteresis of the devices, reducing it over the annealing exposure time. The lower leakage currents presented in sub-section 3.3.2, correspond to the 1-MP capacitors developed at 150 °C assisted by DUV for 30 minutes ($(8.4 \pm 4.2) \times 10^{-7}$ A/cm^2 at 1 MV/cm) and 150 °C assisted by DUV for 60 minutes ($(1.1 \pm 0.9) \times 10^{-6}$ A/cm^2 at 1 MV/cm), thus DUV treatment contributes for the leakage current attenuation. Overall, capacitors developed at 150 °C assisted by DUV for 60 minutes with 1-MP as solvent presented the most promising electrical properties.

Both capacitors developed in 0.1 M and 0.2 M concentrations exhibited good electrical performances. The 0.1 M devices have better capacitance, breakdown electric field and also some instability in the measurements, due to the low thickness, while the 0.2 M have higher dielectric constant and higher thickness. Considering the thickness between the two kind of devices, was chosen the 0.2 M, once the films are thicker, allowing the application on flexible substrates.

The AlO_x dielectric thin films using 2-ME as solvent and 0.2 M concentration were applied on Kapton successfully, presenting an average leakage current of $(4.6 \pm 6.3) \times 10^{-5}$ A/cm^2 at 0.25 MV/cm. The breakdown electric field was reached at 0.83 MV/cm.

The AlO_x thin films developed, at 300 °C for 30 minutes and at 200 °C assisted by FUV for 30 minutes, with 0.2 M, were applied successfully in solution-based In_2O_3/AlO_x TFTs.

Summarizing, throughout this work realization, it was achieved high quality AlO_x thin films, using eco-friendly solvents and low annealing temperatures.

Hereafter, to further develop this study, it is required new aims, so the next steps to follow are:

- Find the optimal thickness of each previous used solvent by regulating the precursor solution concentration;
- Investigate the dielectric properties over time;
- Develop new thin films with non-health hazardous solvents, with similar properties than 2-ME, for instance other glycol ethers;
- Study the application of the optimized AlO_x dielectrics in TFTs in flexible substrates.

5. References

[1] Y. Kim *et al.*, “Flexible metal-oxide devices made by room-temperature photochemical activation of sol-gel films,” *Letter*, vol. 489, pp. 5–10, 2012.

[2] D. A. Jameel, “Thin Film Deposition Processes,” *Int. J. Mod. Phys. Appl.*, vol. 1, no. August, pp. 193–199, 2015.

[3] E. Carlos, “Oxide transistors produced by solution : Influence of annealing parameters on properties of the insulator,” pp. 1–17, 2015.

[4] E. Carlos *et al.*, “Boosting Electrical Performance of High-κ Nanomultilayer Dielectrics and Electronic Devices by Combining Solution Combustion Synthesis and UV Irradiation,” *ACS Appl. Mater. Interfaces*, vol. 9, no. 46, pp. 40428–40437, 2017.

[5] M. Kim, “Low-temperature fabrication of high-performance metal oxide thin-film electronics via combustion processing,” *Nat. Mater.*, vol. 10, no. 5, pp. 382–388, 2011.

[6] J. M. Chem, C. Avis, and J. Jang, “High-performance solution processed oxide TFT with aluminum oxide gate dielectric fabricated by a sol–gel method,” pp. 10649–10652, 2011.

[7] J. Robertson, “High dielectric constant oxides,” *Eur. Phys. J. Appl. Phys.*, vol. 291, pp. 265–291, 2004.

[8] J. Hwang *et al.*, “UV-Assisted Low Temperature Oxide Dielectric Films for TFT Applications,” *Adv. Mater. Interfaces*, vol. 1, no. 8, pp. 1–9, 2014.

[9] L. Pereira, A. Vilà, and J. R. Morante, “Low-temperature sputtered mixtures of high- κ and high bandgap dielectrics for GIZO TFTs,” 2010.

[10] H. Tan, G. Liu, A. Liu, B. Shin, and F. Shan, “The annealing effects on the properties of solution-processed alumina thin fi lm and its application in TFTs,” *Ceram. Int.*, pp. 1–7, 2015.

[11] X. Ye *et al.*, “High performance low-voltage organic fi eld-effect transistors enabled by solution processed alumina and polymer bilayer dielectrics,” vol. 209, pp. 337–342, 2015.

[12] G. D. Wilk, R. M. Wallace, and J. M. Anthony, “High-κ gate dielectrics : Current status and materials properties considerations,” vol. 5243, no. 2001, 2012.

[13] S. Y. Lee, S. Chang, and J. Lee, “Role of high-k gate insulators for oxide thin fi lm transistors,” *Thin Solid Films*, vol. 518, no. 11, pp. 3030–3032, 2010.

[14] G. X. Liu *et al.*, “High-performance fully amorphous bilayer metal-oxide thin film transistors using ultra- thin solution-processed ZrOx dielectric High-performance fully amorphous bilayer metal-oxide thin film transistors using ultra-thin solution-processed ZrO x dielectric,” vol. 113509, pp. 1–6, 2014.

[15] C. Falcony and G. Alarcon-flores, “Electrical , optical , and structural characteristics of ultrasonic sprayed pyrolysis thin films prepared by pulsed Electrical , optical , and structural characteristics of Al2O3 thin films prepared by pulsed ultrasonic sprayed pyrolysis,” vol. 5243, no. 2001, 2011.

[16] A. Sharma, O. P. Modi, and G. K. Gupta, “Effect of fuel to oxidizer ratio on synthesis of Alumina powder using Solution Combustion Technique-Aluminium Nitrate & Glycine combination,” vol. 3, no. 4, pp. 2151–2158, 2012.

[17] R. Branquinho *et al.*, “Solution based zinc tin oxide TFTs : the dual role of the organic solvent,” *J. Phys. DApplied Phys.*, 2017.

[18] S. K. Singh and A. W. Savoy, “Ionic liquids synthesis and applications: An overview,” *J. Mol. Liq.*, 2019.

[19] F. J. G. Ortiz and A. Kruse, “The use of process simulation in supercritical fluids applications,” *React. Chem. Eng.*, pp. 1–5, 2020.

[20] W. Abdussalam-mohammed, A. Qasem, and A. O. Errayes, “Green Chemistry : Principles , Applications , and Disadvantages,” *Chem. Methodol.*, vol. 4, pp. 408–423, 2020.

[21] C. Capello, U. Fischer, and K. Hungerbu, “What is a green solvent ? A comprehensive framework for the environmental assessment of solvents,” pp. 927–934, 2007.

[22] R. Branquinho, D. Salgueiro, L. Santos, P. Barquinha, R. Martins, and E. Fortunato, “Aqueous Combustion Synthesis of Aluminum Oxide Thin Films and Application as Gate Dielectric in GZTO Solution-Based TFTs,” *Appl. Mater.*, pp. 19592–19599, 2014.

[23] R. Branquinho *et al.*, “Towards environmental friendly solution-based ZTO/AlOxTFTs,” *Semicond. Sci. Technol.*, vol. 30, no. 2, p. 24007, 2015.

[24] “Hadassa Reinskjen Leite do Valle Effect of eco-friendly solvents in solution-based ZrO x dielectrics,” 2019.

[25] “Thin-Film Transistor Fabricated in Single-Crystalline Transparent Oxide Semiconductor Author (s): Kenji Nomura , Hiromichi Ohta , Kazushige Ueda , Toshio Kamiya , Masahiro Hirano and Hideo Hosono Source : Science , New Series , Vol . 300 , No . 5623 (May 23 , 2003), pp . 1269-1272 Published by : American Association for the Advancement of Science Stable URL : http://www.jstor.org/stable/3834084,” vol. 300, no. 5623, pp. 1269–1272, 2016.

[26] M. Epifani, E. Melissano, G. Pace, and M. Schioppa, “Precursors for the combustion synthesis of metal oxides from the sol – gel processing of metal complexes,” vol. 27, pp. 115–123, 2007.

[27] P. Gil and D. Trigo, “Oxide transistors produced by Combustion Synthesis : Influence of the PVP on the properties of the insulator,” 2017.

[28] R. Branquinho *et al.*, “Solution Combustion Combustion Synthesis : Application in Oxide Electronics,” *Intech*, pp. 398–417, 2016.

[29] S. L. González-cortés and F. E. Imbert, “Applied Catalysis A : General Fundamentals , properties and applications of solid catalysts prepared by solution combustion synthesis (SCS),” *"Applied Catal. A, Gen.*, vol. 452, pp. 117–131, 2013.

[30] H. Imai *et al.*, “Ultraviolet-reduced reduction and crystallization of indium oxide films Ultraviolet-reduced reduction and crystallization of indium oxide films,” vol. 203, no. 1999, 2010.

[31] E. Carlos, R. Branquinho, A. Kiazadeh, P. Barquinha, R. Martins, and E. Fortunato, “UV mediated photochemical treatment for low temperature oxide based TFTs,” *Appl. Mater. Interfaces*, pp. 1–26, 2016.

[32] J. Leppäniemi *et al.*, “Rapid low-temperature processing of metal-oxide thin film transistors with combined far ultraviolet and thermal annealing Rapid low-temperature processing of metal-oxide thin film transistors with combined far ultraviolet and thermal annealing,” vol. 113514, 2014.

[33] Q. Formula and B. Theorem, *Fundamentals of Phisics*, 9th ed. .

[34] K. Lehovec and L. Sm-t, “ANALYSIS OF C - V DATA IN THE ACCUMULATION REGIME OF MIS STRUCTURES,” *Solid. State. Electron.*, vol. 19, pp. 993–996, 1976.

[35] A. Jakubowski and K. Iniewski, “CHARACTERISTICS OF MIS CAPACITOR,” vol. 26, no. 8, pp. 755–756, 1983.

[36] L. Pereira, “Produção e caracterização de silício policristalino e sua aplicação a TFTs,” 2008.

[37] A. Isabel and B. Santa, “Transístores de óxidos semicondutores com óxido de alumínio produzido por solução,” 2014.

[38] P. Taptimthong, J. Rittinger, M. C. Wurz, and L. Rissing, “Flexible magnetic writing / reading system : Polyimide film as flexible substrate,” *Procedia Technol.*, vol. 15, pp. 230–237, 2014.

[39] N. L. S. L. M. Gonc, “Deposition of conductive materials on textile and polymeric flexible substrates,” pp. 635–643, 2013.

[40] B. C. Zhu, B. Cho, and M. Li, “Atomic Layer Deposited High- j Films and Their Role in Metal-Insulator-Metal Capacitors for Si RF / Analog Integrated Circuit,” pp. 165–171, 2006.

[41] M. Danaie, H. Aminzadeh, and S. Naseh, “On the Linearization of MOSFET Capacitors,” pp. 1943–1946, 2007.

[42] C. H. Ng, K. W. Chew, and S. F. Chu, “Characterization and Comparison of PECVD Silicon Nitride and Silicon Oxynitride Dielectric for MIM Capacitors,” vol. 24, no. 8, pp. 506–508, 2003.

[43] F. F. Vidor, T. Meyers, and U. Hilleringmann, “Flexible Electronics: Integration Processes for Organic and Inorganic Semiconductor-Based Thin-Film Transistors,” pp. 480–506, 2015.

[44] S. J. Kim, S. Yoon, and H. J. Kim, “Review of solution-processed oxide thin-film transistors,” *Jpn. J. Appl. Phys.*, vol. 02, 2014.

[45] L. Zhu, G. He, J. Lv, E. Fortunato, and R. Martins, “Fully solution-induced high performance indium oxide thin film transistors with ZrOx high-k gate dielectrics,” *RSC Adv.*, vol. 8, pp. 16788–16799, 2018.

[46] S. Han, G. S. Herman, and C. Chang, “Low-Temperature, High-Performance, Solution-Processed Indium Oxide Thin-Film Transistors,” *J. Am. Chem. Soc.*, pp. 5166–5169, 2011.

[47] A. Liu *et al.*, “Fully Solution-Processed Low-Voltage Aqueous In2O3 Thin-Film Transistors Using an Ultrathin ZrOx Dielectric,” 2014.

[48] A. M. da Cunha, “Síntese e caracterização de óxidos a base de cobre disperso em suportes com características àcidas para reações de desidratação de glicerol em fase gás,” 2016.

[49] G. Johnston, R. Muenchausen, D. M. Smith, W. Fahrenholtz, and S. Foltyn, “Reactive Laser Ablation Synthesis of Nanosize Alumina Powder,” *Journal*, vol. 75, pp. 3293–3298, 1992.

[50] G. Balakrishnan, S. T. Sundari, R. Ramaseshan, and R. Thirumurugesan, “Effect of substrate temperature on microstructure and optical properties of nanocrystalline alumina thin fi lms,” *Ceram. Int.*, pp. 1–7, 2013.

[51] J. H. Park and K. Kim, “Water adsorption effects of nitrate ion coordinated Al2O3 dielectric for high performance metal-oxide thin- film transistor,” *Jounal Mater. Chem. C*, pp. 7166–7174, 2013.

[52] H. Lee, X. Zhang, J. W. Kim, E. Kim, and J. Park, “Investigation of the Electrical Characteristics of by Solution Processing,” 2018.

[53] J. M. Reyes, M. P. Ramos, C. Zu, W. C. Arriaga, P. R. Quintero, and A. T. Jacome, “Chemical and Morphological Characteristics of ALD Al2O3 Thin-Film Surfaces after Immersion in pH Buffer Solutions,” vol. 160, no. 10, pp. 201–206, 2013.

[54] "Safety data sheet 100859," 2018. [Online]. Available: https://www.merckmillipore.com/PT/en/product/msds/MDA_CHEM-100859?Origin=SERP. [Accessed: 04-Mar-2021].

[55] "Safety data sheet 116738," 2020. [Online]. Available: https://www.merckmillipore.com/PT/en/product/msds/MDA_CHEM-116738?Origin=SERP. [Accessed: 04-Mar-2021].

[56] "Safety data sheet 100983," 2020. [Online]. Available: https://www.merckmillipore.com/PT/en/product/msds/MDA_CHEM-100983?Origin=SERP. [Accessed: 04-Mar-2021].

[57] E. R. Adlard, "Francesca M . Kerton and Ray Marriott : Alternative Solvents for Green Chemistry , 2nd Edition," pp. 1249–1250, 2014.

[58] W. Yang, K. Song, Y. Jung, S. Jeong, and J. Moon, "Solution-deposited Zr-doped AlOx gate dielectrics enabling high-performance flexible transparent thin film transistors," *J. Mater. Chem. C*, pp. 4275–4282, 2013.

[59] Y. Gong, K. Zhao, H. He, W. Cai, and N. Tang, "Solution processable high quality ZrO2 dielectric films for low operation voltage and flexible organic thin film transistor applications."

[60] G. X. Liu *et al.*, "Annealing Dependence of Solution-Processed Ultra-Thin ZrOx Films for Gate Dielectric Applications," vol. 15, no. 3, pp. 2185–2191, 2015.

[61] W. Xu, H. Wang, F. Xie, J. Chen, H. Cao, and J. Xu, "Facile and environmentally friendly solution-processed aluminum oxide dielectric for low-temperature, high-performance oxide thin-film transistors," *Appl. Mater. Interfaces*, 2015.

[62] A. J. Huh, J. Park, and J. Lee, "Effects of process variables on aqueous-based AlOx insulators for high-performance solution-processed oxide thin-film transistors," *J. Ind. Eng. Chem.*, 2018.

[63] V. A. Online, "The role of solution-processed high- k gate dielectrics in electrical performance of oxide," *J. Mater. Chem. C*, pp. 5389–5396, 2014.

[64] K. C. Patil, S. T. Aruna, and T. Mimani, "C ombustion synthesis : an update," *Elsevier*, vol. 6, no. 2002, pp. 507–512, 2003.

[65] S. R. Jain and K. C. Adiga, "A New Approach to Thermochemical Calculations of Condensed Fuel-Oxidizer Mixtures," vol. 79, pp. 71–79, 1981.

[66] R. Chen and L. Lan, "Solution-processed metal-oxide thin film transistors: a review of recent developments," *Accept. Manuscr.*, 2019.

6. Annexes

Annex A – Solution Combustion Reactions

The aluminum oxide materials were prepared by solution combustion synthesis (SCS). Aluminum oxide results by different molar stoichiometric (1:2.5) of aluminum nitrate nonahydrate, as oxidizer and urea acting as fuel. The balance between aluminum nitrate reduction reaction and the urea oxidation reaction is on table 6.1. [16], [64]

Table 6.1 – Reduction, oxidation and overall reactions

Reduction reaction	
Aluminum nitrate nonahydrate	$2Al(NO_3)_3 \cdot 9H_2O \rightarrow Al_2O_3 + 18H_2O + 3N_2 + \left(\frac{15}{2}\right)O_2$
Oxidation reaction	
Urea	$CO(NH_2)_2 + \left(\frac{3}{2}\right)O_2 \rightarrow 2H_2O + CO_2 + N_2$
Overall reaction	
Aluminum nitrate nonahydrate + Urea	$2Al(NO_3)_3 \cdot 9H_2O + CO(NH_2)_2 \rightarrow Al_2O_3 + 20H_2O + CO_2 + 4N_2 + 6O_2$

To ensure redox stoichiometry amounts of the reaction, it is necessary to calculate the fuel to oxidizer ratios by the following equation: [65]

$$\varphi = \frac{RV}{OV} n \leftrightarrow n = 1 \times \frac{OV}{RV} \quad (4)$$

In the equation (4), reducing valence (RV) and oxidizing valence (OV) correspond to the valency of the reducing reagent and the oxidizing reagent, respectively, $\boldsymbol{n}$ represents the number of moles of fuel per mole of oxidant. The redox stoichiometry is the ideal when φ = 1, which represents that is not required more molecular oxygen for the reaction being completed.[3], [29] Table 6.2 exhibits the valency of the reagents.

Table 6.2 - Valency of the reagents

Reagents	Chemical Formula	Calculation	Total
Oxidizing valence (OV)	$Al(NO_3)_3$*	3 + (3 x 0) + (3 x 3 x -2)	-15
Reducing valence(RV)	$CO(NH_2)_2$	4 -2 + (2 x 0) + (2 x 2 x 1)	+6

* Hydration water does not affect the overall compound valence

When the OV and RV are substituted in the equation (4) by the respective numbers, it is obtained $\boldsymbol{n}$ = 5/2. Table 6.3 presents the correct number of moles of the aluminum precursor.

Table 6.3 – Number of moles (n) to guarantee the redox stoichiometry.

Precursor	φ	Fuel	$\boldsymbol{n}$
Aluminum nitrate nonahydrate	1	Urea	$\left(\frac{5}{2}\right)$

Either reducing or oxidizing valency magnitudes appear as numerical coefficients for balance the oxidizer and the fuel for stoichiometric balance. The overall reaction for the equation stoichiometrically balanced is exhibited in the table 6.4.

Table 6.4 - Overall reaction stoichiometrically balanced

Precursor	Fuel	Overall Reaction
Aluminum nitrate nonahydrate	Urea	$2Al(NO_3)_3 + 5CO(NH_2)_2 \rightarrow Al_2O_3 + 10H_2O + 5CO_2 + 8N_2$

Annex B – MIS and MIM Schematic Procedures

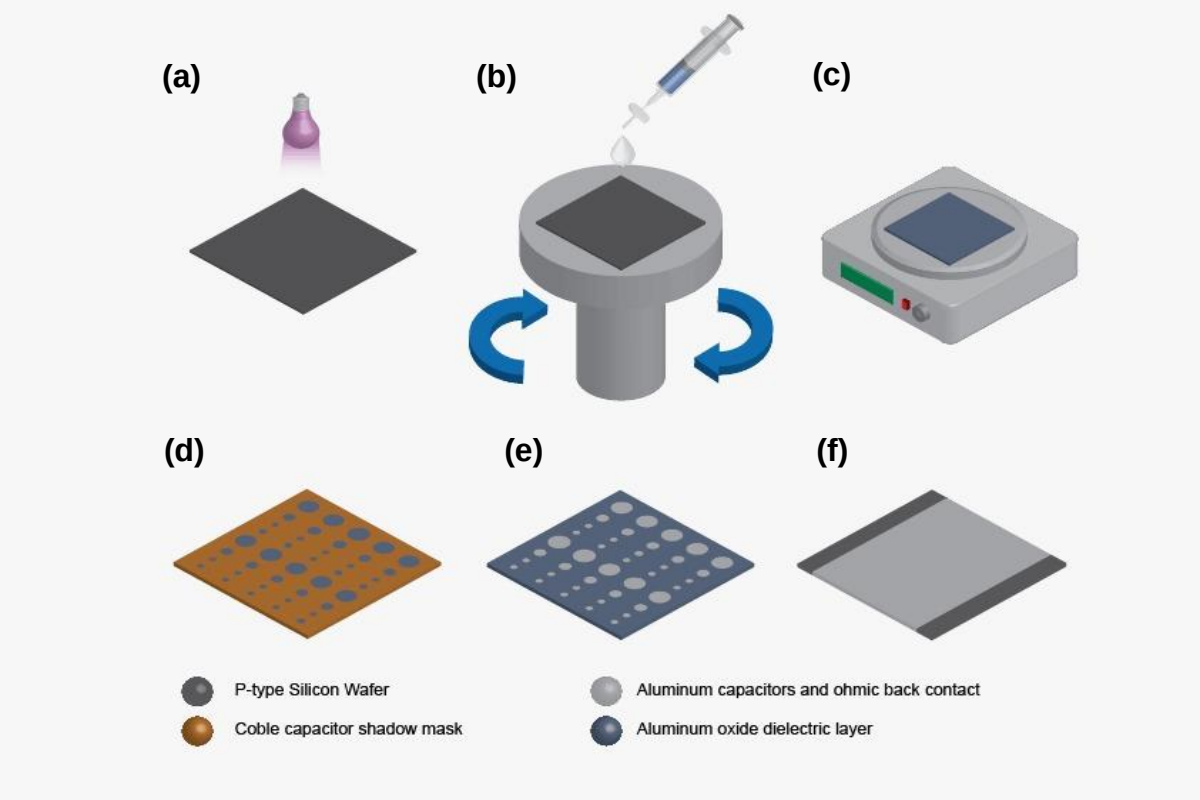

Figure 6.1 – Fabrication procedure of MIS capacitors after cleaning the substrate; (a) UV treatment on the p-type silicon wafer for 15 minutes; (b) Deposition of the precursor solution on the substrate and use the spin coating to spread the solution; (c) condensation and further densification by the annealing step; (d) Deposition of aluminum contact capacitors through the thermal evaporator resorting to a shadow mask; (e) Deposited aluminum contacts after remove the shadow mask; (f) Ohmic back contact deposition by thermal evaporation.

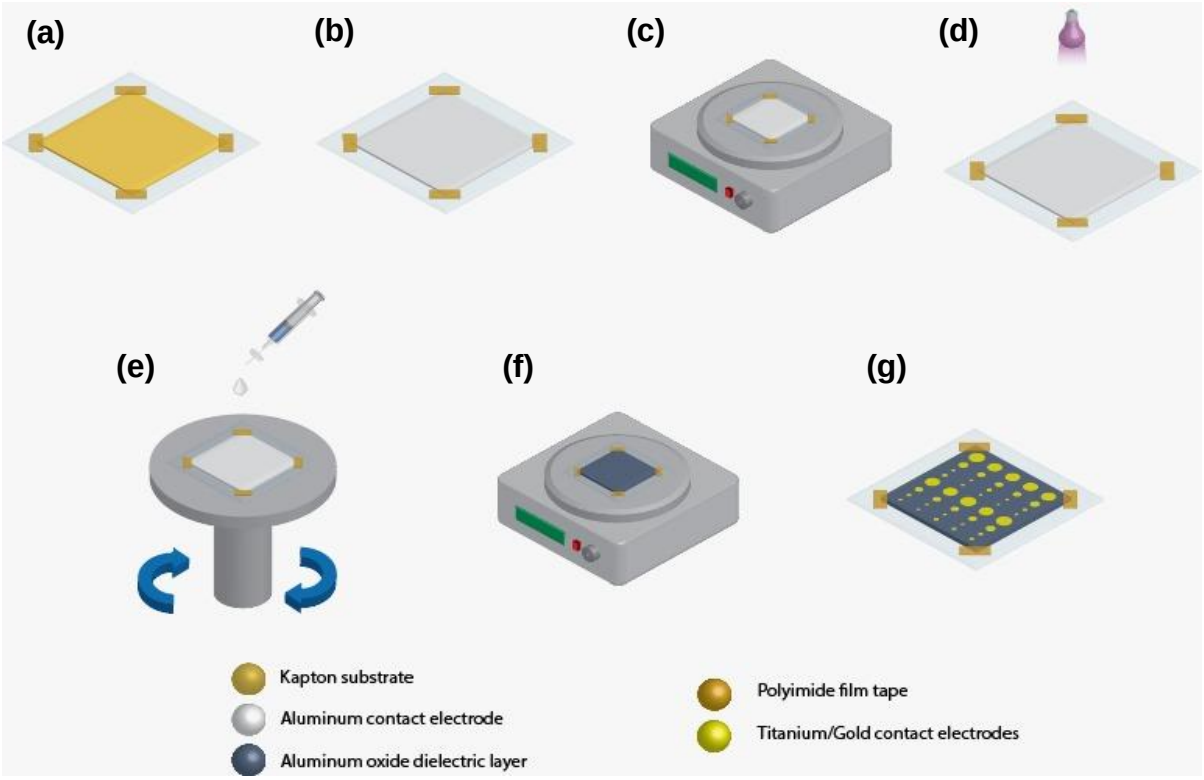

Figure 6.2 - Fabrication procedure of MIM capacitors after cleaning the substrate; (a) Attach the Kapton substrate to a glass with polyimide film tape; (b) Deposit the aluminum contact electrode by thermal evaporation; (c) Submit the Kapton to an annealing step of 180 °C for 10 minutes to avoid shrinking; (d) UV treatment for 15 minutes; (e) Deposit the precursor solution and spread it by spin coating; (f) condensation and further densification by the annealing step; (g) Deposition of the Ti/Au capacitor contacts by E-beam evaporation.

Annex C – Optical Microscopy Analysis

The sample presented in the figure 6.3 showed that after the annealing process the 1-butanol solution did not achieve a thin film homogeneity, once it was obtained a cracked thin film. In these conditions is no further tests were performed.

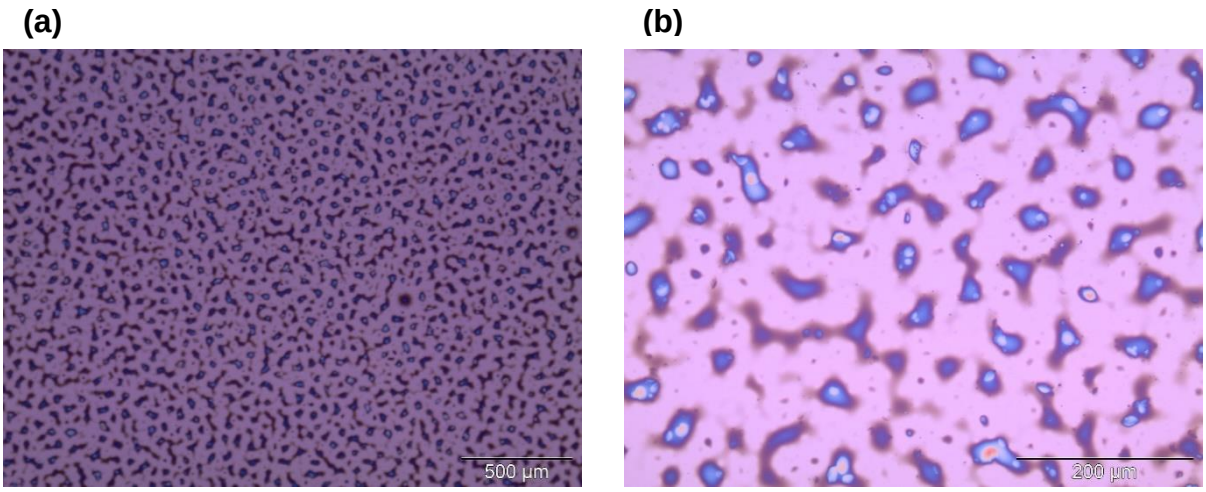

Figure 6.3 – AlO_x thin film obtain at optical microscope using 1-Butanol as solvent after an annealing of 150ºC + DUV for 60 minutes with (a) 5x ampliation and (b) 20x ampliation.

The annealing conditions applied were 150 °C assisted by DUV irradiation for 60 minutes. The time used was 60 minutes to make sure all the organics removal.

Annex D – Ethanol Solutions with 0.1 M

The solution produced using ethanol as solvent, urea as a fuel and aluminum nitrate with a 0.1 M concentration was not used to move to the spin-coating step. In the figure 6.4 is possible to observe 2 blurred solution. The solution on the left with 1 week and the solution on the right removed from the stirrer at that moment. The explanation could be related to the formation of hydroxyl groups (OH).

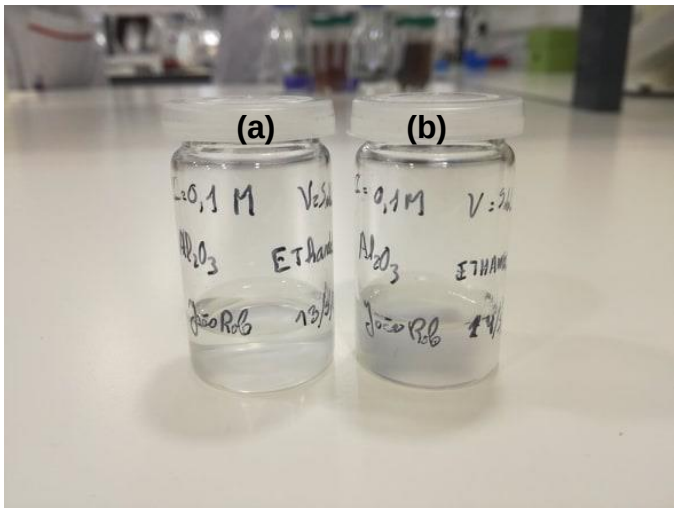

Figure 6.4 - AlO_x precursor solution using ethanol as solvent (a) 1 day after stirring; (b) as-stirred.

Annex E – Solution Concentration using 300 °C for 30 min

The capacitance-frequency, capacitance-voltage and current density–electric field are exhibited for capacitors developed at 0.2 M and 0.1 M concentration at 300 °C for 30 min. In figure 6.5 are shown the electrical characteristics (Cf and CV) of the capacitors developed with 2-ME as solvent.

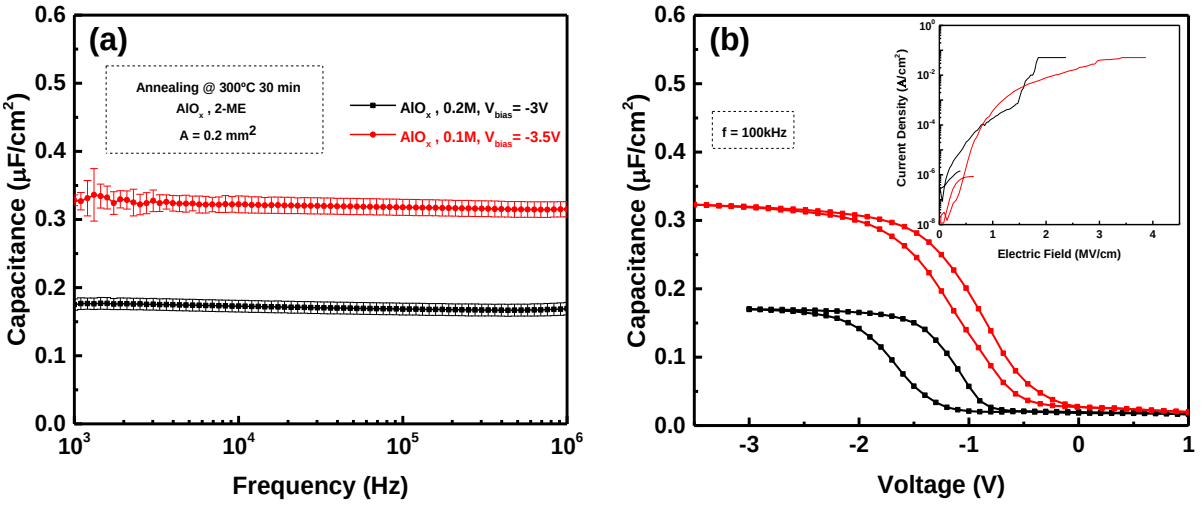

Figure 6.5 - Electrical characterization of AlO_x capacitors 2-ME solution-based, with 0.2 mm^2 of area and different concentrations (0.1 M and 0.2 M), annealed at 300 °C for 30 minutes. (a) Cf curve; (b) CV curve at 100 kHz and JE curve on the inset.

In figure 6.6 are presented the electrical characteristics of the capacitors using 1-MP as solvent.

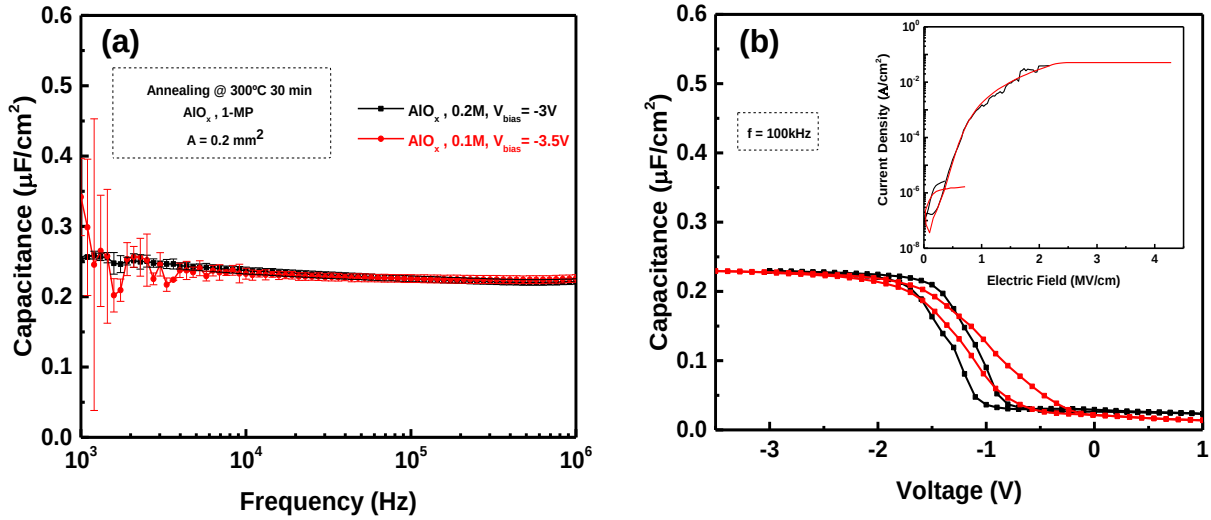

Figure 6.6 - Electrical characterization of AlO_x capacitors 1-MP solution-based, with 0.2 mm^2 of area and different concentrations (0.1 M and 0.2 M), annealed at 300 °C for 30 minutes. (a) Cf curve; (b) CV curve at 100 kHz and JE curve on the inset.

Annex F – Surface Roughness

Through Atomic Force Microscopy (AFM) was possible to obtain the roughness of the inside and outside surface of the used Kapton with a thickness of 75 µm. Figure 6.7 demonstrates the inside surface presents high roughness, for that reason, thin films should be deposited on the outside surface.

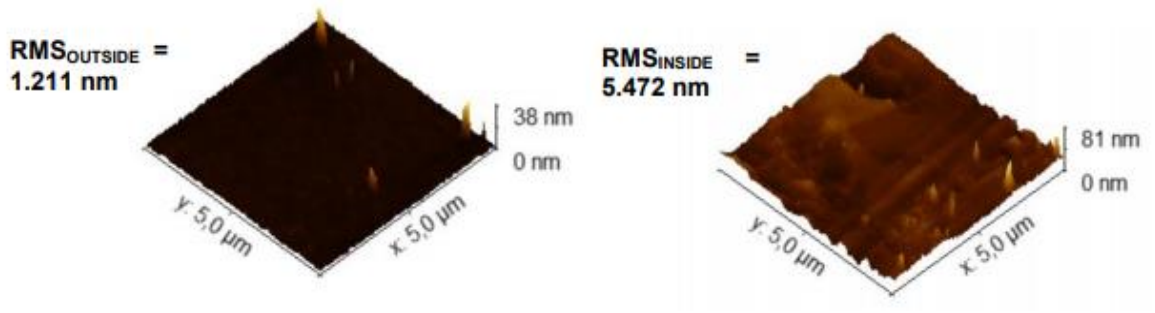

Figure 6.7 - Inside and outside roughness of polyimide substrate obtained by atomic force microscopy.

To comprehend the effect of the annealing conditions, was measured the roughness of polyimide after an annealing of 150 °C assisted on DUV for 30 minutes. After the annealing the outside surface annealed (figure 6.8 (a)) exhibits a roughness considerably higher than the normal conditions surface (figure 6.8 (b)).

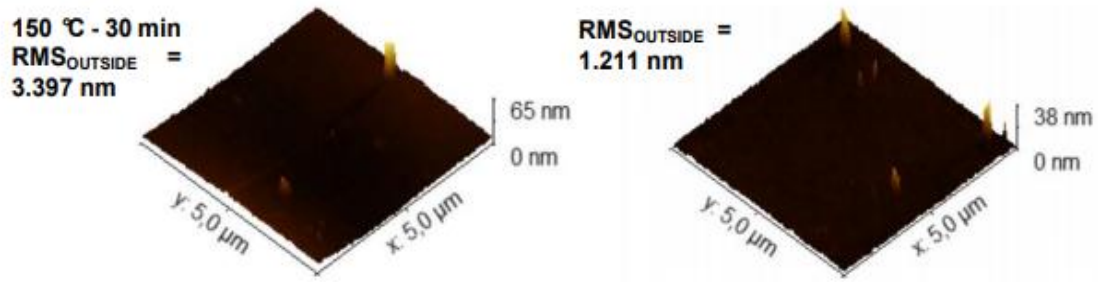

Figure 6.8 - Roughness of outside surface of Kapton substrate after (a) an annealing of 150 °C assisted on DUV for 30 min; (b) no annealing.

Annex G – TFTs annealed at 200 °C assisted by FUV for 30 min

The electric characterization of the dielectric layer used on TFTs application are presented in figure 6.9.

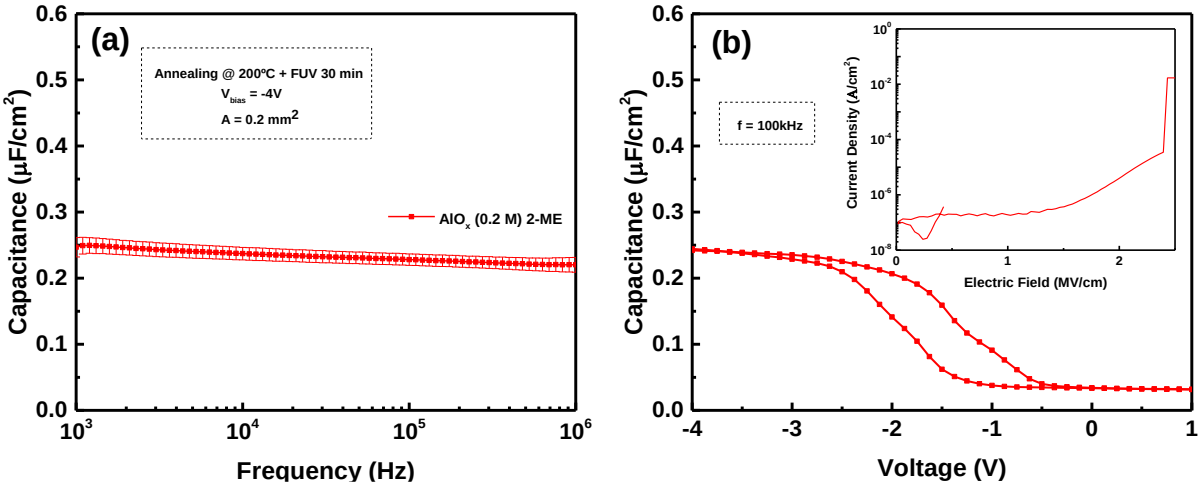

Figure 6.9 - Electrical characterization of AlO_x capacitors 2-ME solution-based, with 0.2 mm^2 of area and 0.2 M, annealed at 200 °C assisted by FUV for 30 minutes. (a) Cf curve; (b) CV curve at 100 kHz and current density (J) curve on the inset.

Table 6.5 summarizes the electrical characterization values.

Table 6.5 - Electrical and physical properties of AlO_x thin film capacitors using 2-ME as solvent, annealed at 200 °C assisted by FUV for 30 minutes with 0.2 M

Condition	Solvent	c (M)	C (nF/cm²) at 1kHz	Thickness (nm)	κ at 1kHz	E (MV/cm)	J (A/cm²) at 1MV/cm
200°C + FUV, 30 min	2-ME	0.2	247 ± 15	23.6 ± 0.1	6.6 ± 0.4	2.43 ± 0.02	(2.0 ± 0.4) x 10^{-7}